Fall 12-10-2016

Compliant Culture Platforms with Independently Tunable Stiffness and Electrical/Optical Functionality

Nadeem Abdul
University of New Mexico - Main Campus

NADEEM ABDUL

Candidate

Electrical and Computer Engineering (ECE)

Department

This thesis is approved, and it is acceptable in quality and form for publication:

Approved by the Thesis Committee

Dr. Francesca Cavallo, Chairperson

Dr. Andrew P. Shreve

Dr. Mani Hossein-Zadeh

Compliant Culture Platforms with Independently Tunable Stiffness and Electrical/Optical Functionality

by

Nadeem Abdul

B.E., Electrical Engineering, Osmania University, 2013

THESIS

Submitted in partial fulfilment of
Requirements for the Degree of

Master of Science
Electrical Engineering

at

The University of New Mexico

Albuquerque, New Mexico

December, 2016

Dedicated to Dr. Francesca Cavallo.

Compliant Culture Platforms with Independently Tunable Stiffness and Electrical/Optical Functionality

by

Nadeem Abdul.

B.E., Electrical Engineering, Osmania University, 2013

M.S., Electrical Engineering, University of New Mexico, 2016

ABSTRACT

Interfacing biological cells and solid-state devices is crucial in many applications, ranging from well-established fields, such as electrophisiology, to the newly developed areas of optogenetics and mechanobiology. Most biological cells are anchored to substrates with elastic modulus, *E*, in the range of ~1 to 100 kPa, the moduli of brain-tissue and osteoid, respectively. On the other hand, bulk semiconductor substrates have ~6 orders of magnitude higher elastic modulus. This large elastic mismatch between devices and cells natural microenvironments is an issue for bio-devices integration, as cells are highly sensitive to mechanical cues. Specifically, cells exert traction forces on their surroundings and adjust their adhesion mechanism, cytoskeleton, locomotion and overall state according to the stiffness of the substrate they are anchored to. This type of behavior makes it a significant challenge to integrate semiconductor devices with biological cells without altering the cell state.

I demonstrate a new family of culture platforms to successfully integrate biological cells and electronic/photonic devices from a mechanical perspective. The proposed platforms are referred to as effectively compliant layered substrates (ECLS). ECLS are based on inorganic nanomembranes (NMs) partially suspended

or bonded to compliant substrates. The unique attribute of ECLS is that, the constitutive material of the NM provides the electrical and optical functionality necessary to a device operation, while the NM geometry and the nature of the supporting substrate can be tailored to match the mechanical response of biological tissues. Specifically, I present fabrication and bio-interfacing of ECLS comprising of device-grade, single-crystal Si NMs on a compliant PDMS substrate with tunable elastic modulus from ~kPa to ~MPa. NMs with thickness in the range of ~20-220 nm and ~ 1x1 cm^2 lateral areas are used in this study. ECLS are obtained using a two-step process, including synthesis of the compliant supporting substrate and fabrication, release and transfer of the NM onto the compliant host. Characterization of the mechanical properties of the ECLS and of the bare compliant substrate is performed by nanoindentation.

Finally, I access a 3T3 fibroblast cell culture on the fabricated ECLS, as well as on bulk silicon and bare soft substrates to investigate cell response to mechanical cues. Specifically, I investigate cytotoxicity of ECLS substrate and conduct a comparative analysis of cell proliferation, morphology, and adhesion mechanisms between bulk Si, and Si-based ECLS with different elastic moduli. Flow-cytometry, bright-field and confocal fluorescence microscopy are used for this study. The proposed ECLS approach has successfully allowed fabrication of device-graded platforms with varying elastic modulus over three orders of magnitude and matching the mechanical properties of a wide range of biological tissues. Fabricated ECLS allowed healthy bioactivity of 3T3 fibroblast with no toxic behavior. 3T3 fibroblast cultured on ECLS with different elastic modulus displayed a drastic change in cytoskeleton (size and shape) and adhesion mechanisms (stress fiber organization and focal adhesions) compared to that of bulk Si.

Acknowledgements

I would like to thank my advisor Prof. Francesca Cavallo for providing me with the opportunity to join in her research group. I also would like to thank Francesca for giving me the freedom to make mistakes, explore, learn and become a more complete and mature researcher/individual. Experience with you will be one of the biggest contributions to my career and life in general. You have been an excellent teacher and the challenge of living up to your standards of excellence was a rewarding experience. I have benefited greatly from my association with all past and present members of the Dr. Cavallo's lab and Grad students at CHTM, in particular Vijay Saradhi Mangu, Mahmoud Behzadirad, Sami Adnan Nazib, Noel Dawson, Denies Torres, Aneesha Kondapi, Farhana Anwar, Marziyeh Zamiri Corey Carlos, and Kenneth Opheim. Interactions with you guys made me a more complete individual.

I would also like to thank Ali Nematollahisarvestani and Prof. Mehran Tehrani from mechanical engineering department for their valuable contribution in this work. A simple thank you is insufficient for Matthew Rush, as he was my mentor in an unknown realm of tissue culture study, without him I would not have accomplished nearly as much in this thesis. I am grateful to Dr. Andrew P. Shreve for providing us with his brightest student and also for his timely critical assessment of proof of plan in tissue culture study.

Last but not least, I would like to thank all staff of CHTM cleanroom and students from CBME, who saved me tremendous amount of time in many experiment by providing timely troubleshoots, tweaks and tricks. Finally, I would like to thank my family and friends for their unconditional support and love.

Table of Content

LIST OF TABLES

LIST OF FIGURES

Chapter 1: Introduction

Bio-device integration

Interfacing solid-state devices and biological entities has enabled a great deal of progress in biomedical science and healthcare since Galvani's first discovery that nerves and muscles could be electrically stimulated (1760s). Pacemakers, neuromodulators, electrophysiology, and cochlear implants are only a few examples signifying the tremendous impact of bio-device integration on our quality of life. Miniaturization of inorganic materials and solid-state devices has further extended the scope of electronics, opto-electronics, and photonics towards bio-applications. As a result, a variety of micro- and nanoscale devices are increasingly being used for therapy-delivery, diagnostics, prosthetics, fundamental research, and tissue engineering. Figure 1 shows several examples of electronic devices for in vivo applications.

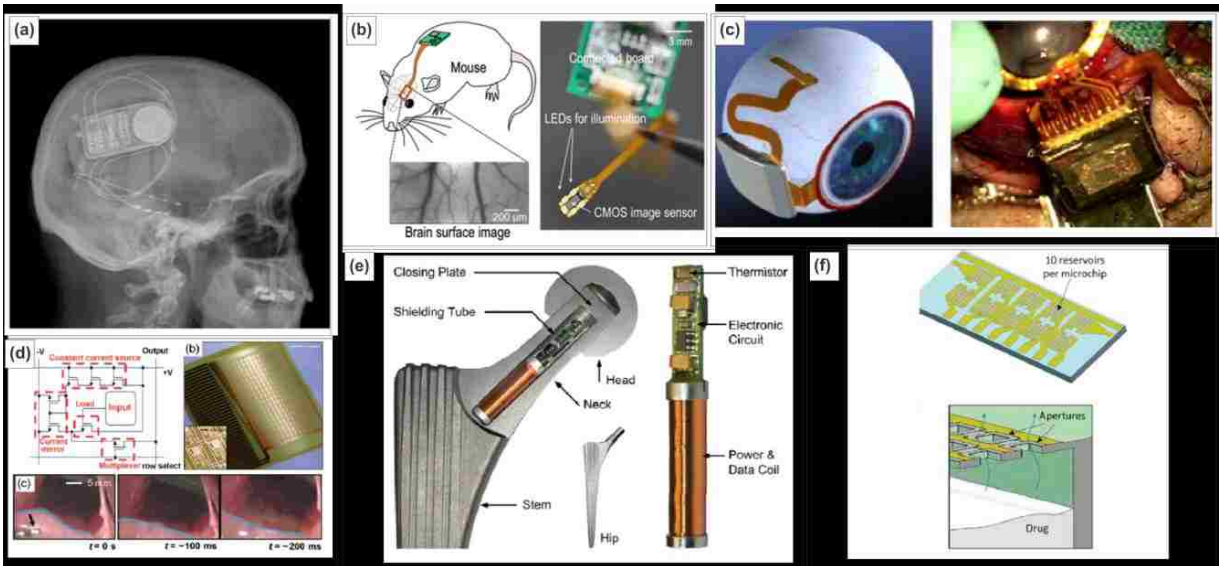

Figure 1.1: (a) Closed loop responsive neurostimulation. (b) Monitoring brain activity and action of a mouse using micro-photonic. (c) Retinal prosthesis: schematic version and a photograph of an implant. (d) An active, flexible device for cardiac electrophysiological mapping (e) Cross-section of a model of the modified hip implant with a metal head. (f) The implantable microchip-based human parathyroid hormone drug delivery device.

Despite the recent advancement in Micro-electro-mechanical systems (MEMS) and microfluidic lab-on-chip biomedical systems for development of devices for rapid diagnostics, and precisely controlled delivery of drugs and complex therapeutics, a successful bio-device integration still face various challenges related to interfacing biological entities and device designs. Biological cells are extremely sensitive to their microenvironment; an implanted device with chemically harsh environment can result in change in growth factors and cell state. On the other end of spectrum, the bio degradation of implanted device and its by-products may stimulate activation of a range of immune mechanisms, leading to inflammation, toxic leach out which further hinder the recovery of damaged tissues. Surface fouling and infections are also of great concern. Biological cells not only respond to chemical microenvironment, but they are also capable of detecting dissimilar mechanical surrounding from that of their own. By process of mechanotransduction, the mechanical stimuli are detected and transferred as chemical signals that cells can process and respond to. Mechanical mismatch between biological tissue and device material has shown to affect the inflammatory response of biological tissues. In an attempt to remove the foreign body, cells release a host of chemical and biological factors that contribute to localized cell degeneration and cell death. One of the mechanical properties of a substrate that can affect cellular behavior is known to be stiffness, mostly measured by elastic modulus. Biological cells modulate their behavior, express by changing cell shape, adhesion to substrate, proliferation, and differentiation in response to mechanical stimuli, knowledge of which is essential for adequate device design.

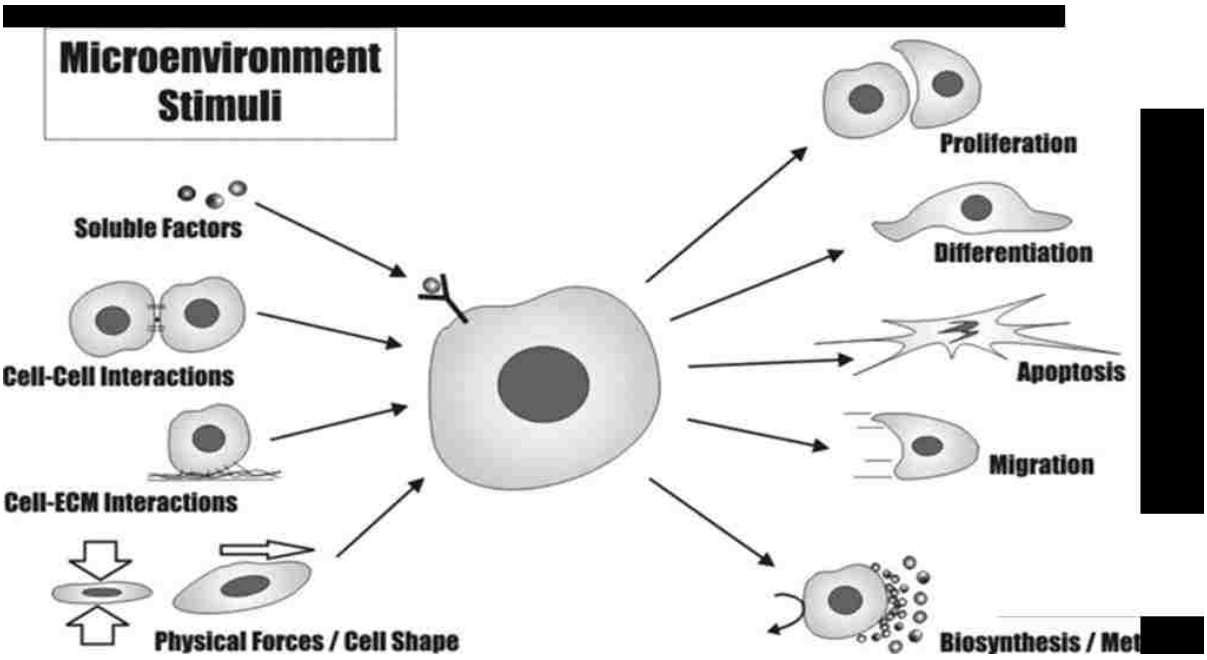

Figure 1.2: Schematic illustrates change in cell behavior due microenvironment stimuli

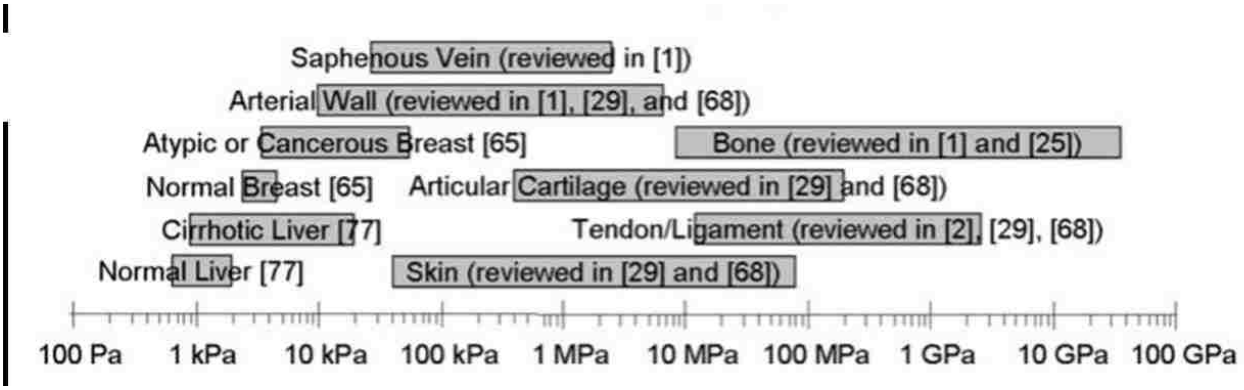

Figure 1.3: Capture substrate anchored cell behavior studied in literature

Conventional electronic/ optical devices implanted in human body are made out of silicon based technology, bulk semiconductor substrates have 6order of magnitude higher elastic modulus compared to that of a typical biological cells environment. For most biological cells, silicon based device can turn out to be highly unfavorable microenvironment owing to their mechanical rigidity. Most biological

cells are anchored to substrates with elastic modulus, E, in the range of ~1 to 100 kPa, the moduli of brain-tissue and osteoid, respectively. On the other hand, bulk semiconductor substrates have ~6 orders of magnitude higher elastic modulus. This large elastic mismatch between devices and cells natural microenvironments is an issue for bio-devices integration, as cells are highly sensitive to mechanical cues. Specifically, cells exert traction forces on their surroundings and adjust their adhesion mechanism, cytoskeleton, locomotion and overall state according to the stiffness of the substrate they are anchored to.

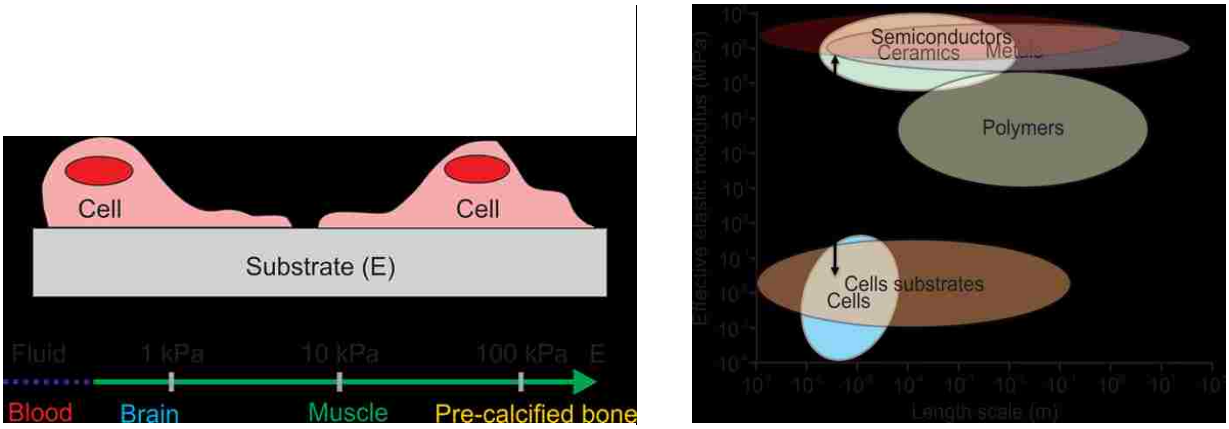

Figure 1.4: a) biological cells anchoring elastic modulus in their native environment b) highlights the existing mismatch between cell-device mechanical environments.

Current study is a major step forward in the direction of developing electronic/photonic devices in biological environment from a mechanical perspective. In this thesis, I demonstrate a new family of culture platforms to successfully integrate biological cells and electronic/photonic device material. The proposed platforms are referred to as effectively compliant layered substrates (ECLS). ECLS are based on inorganic nanomembranes (NMs) partially suspended or bonded to compliant substrates. The unique attribute of ECLS is that, the constitutive material of the NM is an electrically/optically active functional layer

necessary for a device operation, while the NM geometry and the nature of the supporting substrate are designed to match the mechanical response of biological tissues

ECLS approaches were developed to control substrate rigidity in three orders of magnitude. With the underlying premise that device graded compliant platforms could be used to control cell behavior, the objective of this thesis was to rationalize the impact of mechanical properties of bulk silicon and establish the merit for silicon nanomembrane in combination with soft polymers as a platform to achieve control of substrate rigidity in semiconductor materials. The thesis is divided into four chapters (excluding introduction). Chapter 2 provides the detailed methods and characterization techniques employed in this work. It is divided into three sections, Section 1 introduces fabrication of the effectively compliant layered substrates (ECLS); containing fabrication of compliant substrate: Polydimethylsiloxane (PDMS), PDMS modification for biocompatibility, and Silicon Nano membrane (Si NM) fabrication and integration with the compliant host. Section 2 provides details on characterization of the effectively compliant layered substrates (ECLS) using techniques like contact angle measurements for wettability; and Nano indentation/ Atomic-force microscopy (AFM) for mechanical characterization of compliant base and ECLS substrates. Section 3 introduces *In vitro* study: cell culture protocol and cell characterization methods like flow cytometry for cell viability and cell proliferation and confocal microscopy for Immunofluorescent staining of cytoskeleton structure. Chapter 3 presents the rationale for ECLS approach derived from previous theoretical study. Presents results of various formulations of Polydimethylsiloxane (PDMS) investigated. Results include approach implemented in synthesis of PDMS as a novel polymer that maximizes the power of mechanical tunablity with simple

modifications in the process. Wettability of PDMS formulation and elastic modulus of substrates is presented. In section 2, I present various ECLS fabricated by implementing different configuration of Si NM. Chapter 4 starts with introduction of 3T3 fibroblast in *In vitro* study. I present results on cell viability; cell proliferation on Si-based ECLS platform in comparison with bulk silicon. In final section cell expression such as cell shape, focal adhesion, fiber organizations associated with substrate rigidity studied on ECLS and bulk silicon are presented.

Chapter 2: Experimental Methods

In this chapter, I discuss various experimental techniques employed in my research study. The first part of chapter 2 deals with, fabrication and characterization methods of effectively compliant layered substrates. Synthesis of the compliant substrate of choice is described. Various approached to integrate thin semiconductor layers are presented. Methods to characterize the structural properties, as well as the mechanical response and the surface wettability of ECLS and compliant substrates are elucidated. The second part of chapter 2 illustrates methods to evaluate cell response on the fabricated substrates, including sample preparation for *in vitro* studies, the protocol utilized for cell culture, and cell characterization techniques (e.g., flow-cytometry and fluorescence microscopy)

2.1. Fabrication of the effectively compliant layered substrates (ECLS)

ECLS fabrication is a two-step process, involving synthesis of the compliant supporting substrate and fabrication, release and transfer of a thin Si film or nanomembrane (NM) onto the compliant host.

2.1.1. Compliant substrate: Polydimethylsiloxane (PDMS)

Polydimethylsiloxane (PDMS) belongs to the family of polymeric organo-silicone compounds. Its chemical formula is $CH_3[Si(CH_3)_2O]_nSi(CH_3)_3$ where n is the number of repeating monomer $[SiO(CH_3)_2]$ units. In my research work I have used an elastomer-like PDMS, namely Sylgard 184, and a gel-like PDMS or soft silicone, namely Sylgard 527.

PDMS 184 is a two-part elastomer kit with a base and a curing agent. The ratio between the curing agent and the base defines the degree of cross-linking and the elastic modulus of the material. Syglard 527 is a two-part gel kit, used as attenuation to create low stiffness gels of the combined blend. Sylgard 527 gel consists of Part A and Part B dielectric kit. I have used a blend-

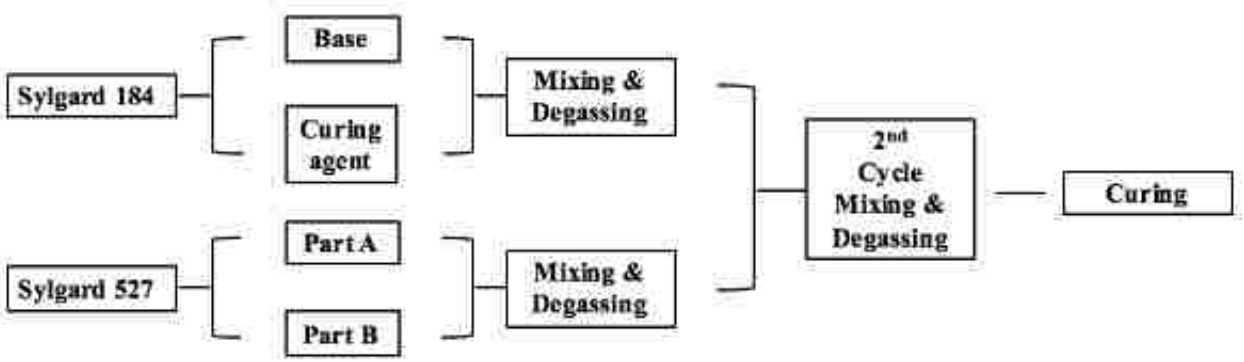

[redacted]

of both 184 and 527 to create hybrid chemically stable PDMS substrates with tunable mechanical properties. The two blends of PDMS (Syglard 527 and Sylgard 184) are mixed in various mass-to-mass ratios. Reference PDMS substrates are prepared using Sylgard 527 only and Sylgard 184 only. Manufacturer's specifications were used in this process. Manufacturer's directions for a Sylgard 184 are

(i) Mixing the base and the curing agent in 10:1 ratio;

(ii) twenty minutes degassing (or defoaming) into a vacuum dessicator;

(iii) Curing at 850C for 4 hours.

Manufacturer's directions for a Sylgard 527 are

(i) Mixing part A and part B in a 1:1 ratio;

(ii) twenty minutes degassing (or defoaming) into a vacuum dessicator;

(iii) Curing at 650C for 12 hours.

Hybrid 527:184 PDMS are fabricated for four different formulations of mass ratios, as reported in detail in Chapter3. The process steps followed to obtain hybrid PDMS substrates is summarized in Figure 2.1. Each blend is made by first preparing pure Sylgard 184 and pure Sylgard 527. Sylgard 527 is prepared by mixing selected weights of part A and part B, followed by a 10 min defoaming cycle. Similarly, pure Sylgard 184 is prepared by mixing selected weights of base and curing agent. The mixture is then placed in a vacuum dessicator for a 20 min defoaming cycle to remove any air bubbles that arise during mixing of the base and curing agent. In the final stage, the two mixtures are blended in the selected mass ratios, followed by an additional defoaming cycle. In each case, once mixed, the PDMS is poured into 150 mm diameter petri dishes to create 1 mm thick films. All hybrid PDMS blends are cured at 65^{o}C for 12 hours. Previous studies have reported that this curing conditions yield a PDMS substrate with stable mechanical properties over time.

2.1.2. PDMS modification

A post-synthesis modification of the PDMS substrates is required to enable fabrication of ECSL and successful *in vitro* studies. Specifically, I utilized Soxhlet solvent extraction to remove uncrosslinked chain in PDMS which may leach out during in vitro studies, thereby creating a toxic environment for biological cells. Uncrosslinked chains are also responsible of the tackiness and hydrophobic nature of the PDMS surface. After Soxhlet solvent extraction, PDMS substrates undergo Ultraviolet (UV)/ ozone treatments to increase wettability of the surface, and hence create a more favorable template for NM transfer and cell culture.

Soxhlet Solvent Extraction

PDMS curing is a time- and temperature-dependent process that does not achieve 100% crosslinking. It has been previously demonstrated that even after extensive curing, as much as 5% (wt/wt %) of the PDMS remains uncrosslinked. Soxhlet solvent extraction removes unreacted molecules in the polymerized PDMS. In my experiments cured PDMS substrates are cut into 20 mm PDMS samples using a punch.

Each PDMS specimen is carefully peeled from the petri dish. Next, PDMS is washed in de-ionized water (DIW) and sandwiched between a filter paper and a non-sticky wipe. Several PDMS samples are piled up and mounted into a glass filter which is then placed in a soxhlet thimble (see Fig. 2.2). This configuration is used to provide support as well as to facilitate handling of the soft materials. My selected extraction solvent (acetone/ n-hexane in 1:1 ratio) is placed in a distillation flask, which is sitting on a hot plate. A reflux condenser is placed atop

the extractor. The solvent is heated to its boiling point (i.e., 130^{o}C). Condensation of the vapor causes the solvent to drip in the thimble containing the PDMS specimens thereby extracting any uncured oligomers from the material. When the thimble or soxhlet chamber is almost full, the chamber is emptied by the siphon.

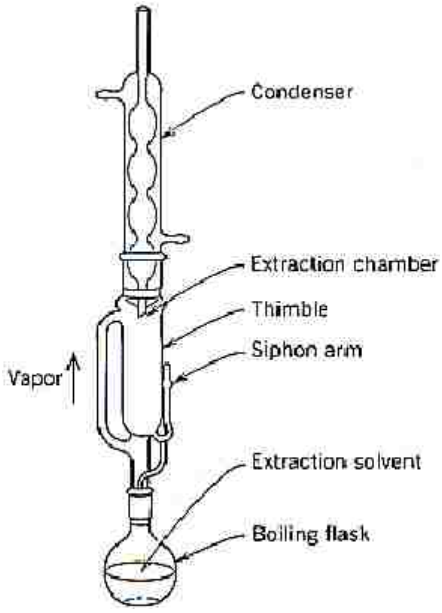

The solvent is returned to the distillation flask. The thimble ensures that the rapid motion of the solvent does not transport any solid material to the distillation flask. Then another extraction cycle starts. After a 3 h long soxhlet extraction I separate the various PDMS specimens, remove the wet filter paper and non-sticky wipe and gently transfer the swollen PDMS to a new set of non-sticky wipe and filter paper. After an overnight air dry under an exhaust hood, samples shrink back to their pre-Soxhlet dimensions and are then transferred on to a 15mm glass coverslip before further processing.

Ultraviolet/Ozone (UVO) Treatment

The ultraviolet/ozone (UVO) treatment of the PDMS surface is used to convert the hydrophobic surface of PDMS into hydrophilic. UVO treatment is a photosensitized oxidation process in which the molecules of the treated material are excited and/or dissociated by the absorption of short-wavelength UV radiation. The surface modification of polymers is accomplished by – functional group implantation. Energetic photons, electrons or ions found in plasma break bonds within the polymer backbone. Carbon-containing fragments leave the surface in the form of volatile organic species, while low-molecular weight polymer chains and

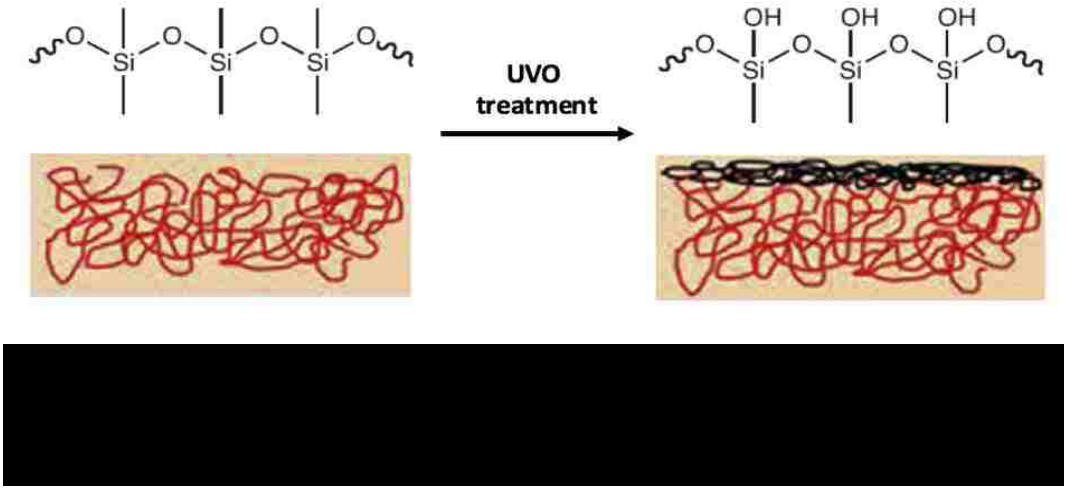

Stable radicals remain on the polymer's surface. The effect of exposing a PDMS surface to UVO is schematically illustrated in Fig. 2.3. In my experiment the process is carried out in a commercial UVO chamber (Jelight Company, Inc., Model 144AX). In this tool, PDMS specimens are placed into the UVO cleaner tray at a distance of about 5 mm from the UV source and they are exposed to the radiation for a controlled period of time. Different amount of treatment times is tested and are reported in detail in Chapter3. It is to be noted that, samples after UVO treatment are stored in water before any further use.

2.1.3. Nano membrane (NM) fabrication and integration with the compliant host

In this section I discuss the fabrication, release, and transfer of nanomembranes (NMs). Typically, NMs are fabricated from multi-layer stacked substrates comprising a functional layer (i.e., the NM) and a sacrificial layer (SL) on a bulk substrate. In this work, we isolate single-crystalline Si NMs from commercially available Si-On-Insulator (SOI) substrates. SOI comprises a Si NM, a SiO_2 sacrificial and a bulk Si substrate (see Fig. 2.4).

Figure 2.4: SOI multilayered structure.

Sample Cleaning

Before any processing, SOI wafers undergo a standard cleaning procedure follows the concept of Shiraki et al and comprising the following steps:

1. 1 min dip in 5% vol HF solution;
2. 3 min rinse in de-ionized water (DIW);
3. 8 min H_2SO_4 (66%):H_2O_2 (33%) dip;
4. 3 min rinse in DIW.

Thermal Oxidation

Thinning of the silicon NM is accomplished by thermal oxidation of the SOI wafer. During thermal oxidation an oxidizing agent is forced to diffuse into the wafer at high temperature and react with silicon, thereby creating a high temperature oxide layer (HTO) on the surface of the SOI wafer (see Fig. 2.5). The rate of oxide growth is predicted by the Deal-Grove model. Next, the SiO_2 is removed from the surface using a HF solution. In this study, thermal oxidation is performed in a horizontal tube furnace operated in 1100^{o}C temperature range under ultra-pure (99.9%) O_2 and N_2 flow.

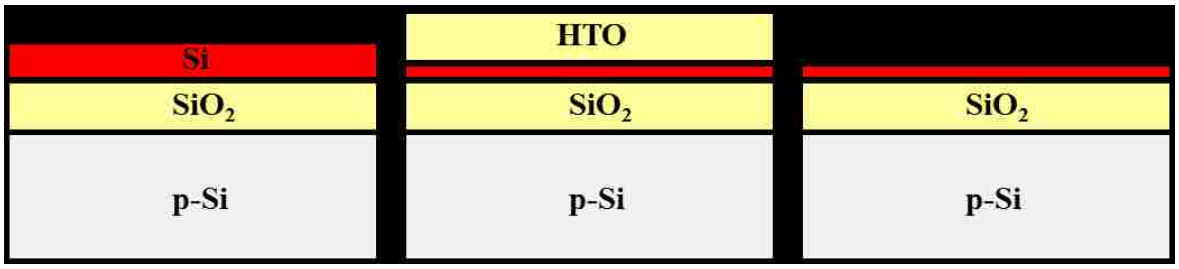

Figure 2.5: Schematic illustration of Si thinning via thermal oxidation and subsequent oxide removal.

Photolithography

Conventional photolithography is used to pattern outline of the membranes onto SOI wafer. The outline of the membrane is imprinted from a custom designed chrome etched mask deposited on quartz glass. Here I have used both a positive (AZ 4330) and an image reversal (AZ5214E) photoresist as per experimental need.

Photolithography	Positive	Negative
Photoresist	AZ4330	AZ5214IR
Sample cleaning	3x Acetone - 1x IPA - N_2 blow dry	
Surface preparation	Hexamethyldisilane (HMDS) spun at 5000rpm. Bake at 150° C for 1 min	
Photoresist spin coating	30 sec at 4500 rpm	30 sec at 5000 rpm
Soft-baking	2 min at 90° C	90 sec at 90° C
UV light exposure	8-10 sec	
Post-exposure baking	-	60 sec at 112° C
Flood exposure (No mask)	-	30 sec
Developer	Dip in AZ400K for ~50 sec;	
Sample finishing	Rinse with water and N_2 blow dry	

Table 2.1: Photolithographic process used to transfer a pattern on to the photoresist surface

The photoresist-covered sample surface is brought into contact with chrome mask and is exposed for a predefined time under UV lamp using a contact lithography mask aligning system (Karl Suess MJB-3). The pattern is later developed under AZ400k base developer solution. A detailed description of the photolithographic processes used in my work is reported in Table 2.1.

The pattern impressed on the photoresist by lithography is transferred to the silicon template by reactive-ion etching. In this process a reactive chemical gas interacts with the surface by using a combination of chemical and physical etching processes. Etch gas atoms are accelerated toward the substrate by a large radio frequency (RF) voltage, and upon contact chemically react with the surface while also physically removing material due to their high kinetic energy. In this work, CF_4/O_2 is used to etch the silicon down to the sacrificial layer (see Fig. 2.6). RIE was performed in a Plasmalab μP system at 100 W and chamber pressure of 15 mTorr. The etching rate of Si was estimated to be 30 nm/ min in these conditions.

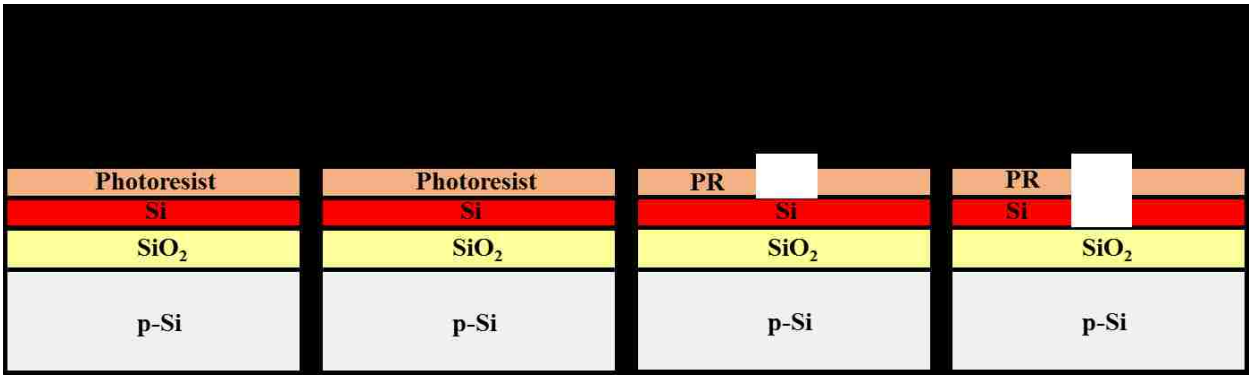

Figure 2.6: Schematic illustration of photolithography and RIE.

After RIE photoresist was removed by a dip in acetone cleaning, followed by a 10 min treatment in a nano-stripper solution at 80°C. Additional treatments like oxygen plasma or conventional 1:3 piranha solution are performed if necessary.

Membrane release

Release of the membrane is accomplished by selective etching of the SiO_2 sacrificial layer in hydrofluoric acid (HF). The release time depends on the geometry and lateral size of the NM. In this study, we have used perforated membranes to enhance the access of the etching solution to the sacrificial layer, which results in a faster membrane release.

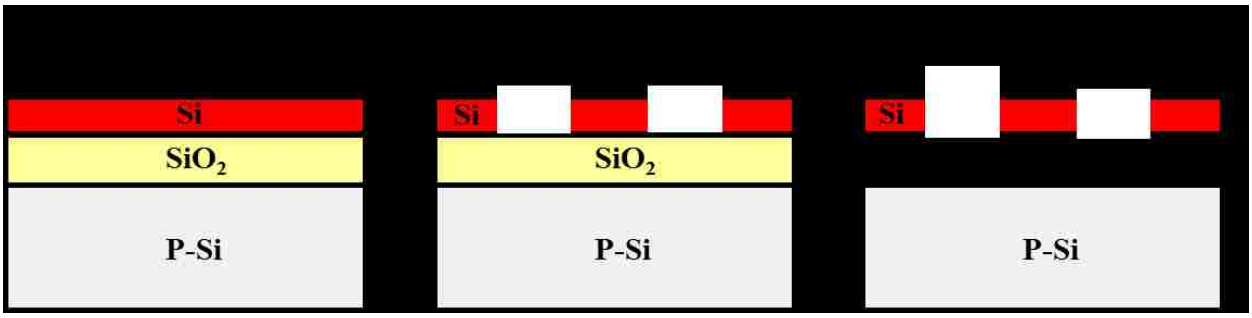

Figure 2.7: Schematic illustration of silicon nanomembrane release from SOI wafer.

To successfully release a membrane employing selective etching process one needs to understand that the etching process is diffusion-limited, not only by the HF reaching the SiO_2 etch front, but by the out-diffusion of hydrogen gas, a by-product of the etching reaction. When the undercut channel increases in length, the etch rate slows down as it is more likely that the hydrogen gas become supersaturated and form bubbles that may block etchant access to the oxide. In addition to that, if a membrane is extremely thin (<100nm), the membrane may deflect towards and reattach to the substrate.

Complete under etching of the membrane is difficult to ascertain visually. The Teflon containers needed for handling HF are opaque. HF solutions are extremely hazardous and prevent convenient examination outside of a ventilation hood. If removed prematurely from solution, membranes will re-attach to the substrate.

Placing the substrate back into solution rarely reopens the access holes. It is advised to set a minimum time before checking for membrane release. As a general rule of thumb, if the membrane is visible, the etching of the sacrificial layer may not be complete. When membrane is not in direct contact with the substrate, one can see a reflection of color -gold, cyan, magenta, or blue, depending on membrane thickness due to the water, oxide, or bubbles between the membrane and the substrate. If the membrane is completely underetched and hence it is in direct contact with the substrate, it will be much less visible. After complete removal of the sacrificial layer the membrane may float off the bulk Si substrate and become freestanding or it may remain loosely bound to it, a condition called "released in place".

Transfer of membranes

Once a membrane is free-standing or released in place, the goal is to place and strongly adhere the released NM onto the designated new host. The challenge is to maintain the NM planar geometry and structural integrity during the transfer process while promoting a strong adhesion at the NM-substrate interface. Transfer of membranes is one of the trickiest steps by far in fabrication of ECLS, especially as this is done manually. Membranes are fragile; any applied loads due to poor handling may easily tear them off. Also, membranes have a tendency to stick to almost any surface, even Teflon. Once they adhere to a surface, they rarely detach in one piece. Membrane transfer can be accomplished by following two well established techniques i.e. Wet and Dry transfer. Essentially, the transfer process chosen depends on the new host substrate and on the thickness and lateral dimensions of the membrane.

Wet transfer

The key advantage of wet transfer is its ability to maintain the flatness of large-area and ultra-thin NM. A support layer of photoresist can help an ultra-thin membrane with large lateral dimensions to float. In this study, I have used two wet transfer techniques. In one approach the membrane floating at the liquid air/interface is scooped up using the new host substrate (see Fig. 2.8). A reliable transfer of large-area membranes requires the new host to be hydrophilic so that the membrane can simply wick up onto the surface by capillary action.

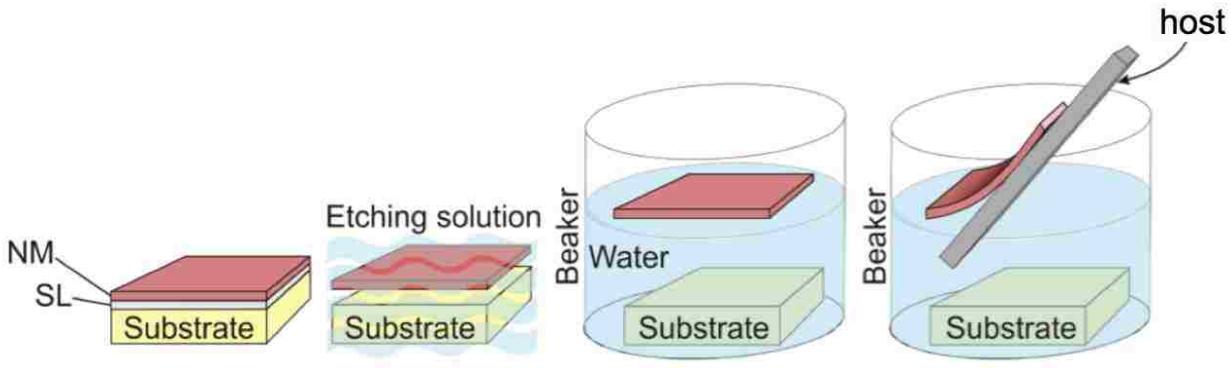

Figure 2.8: Schematic illustration of release and wet transfer of a NM onto a host substrate

An alternative method is to remove the membrane from the solution and transfer it to the substrate using a loop formed out of a Cu- wire of few millimeters in diameter. Across the Cu-loop a liquid film is formed upon dipping into a solution, due to surface tension (see Fig 2.9). The membrane remains suspended on the liquid film

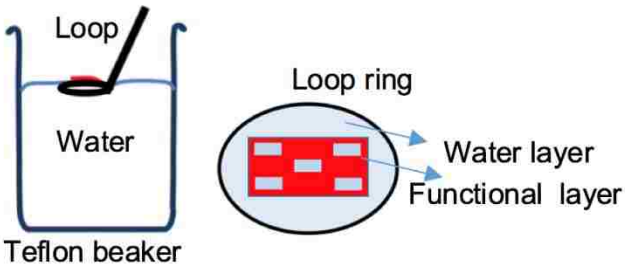

within the loop until it is placed on the new substrate, and the liquid film is dried out using a tissue. Although wet processes are reliable to transfer ultra-thin and large area NMs, they have several disadvantages. Membrane placement on a substrate by wet transfer is gross at best, and interfacial contamination with any solutes is more than likely to occur.

Dry transfer

Dry transfer technique helps mitigate some of the above-mentioned problems from wet transfer. In this study, ECLS are mostly fabricated using dry transfer. A dry transfer simply is a pick-up process that moves the membrane from one substrate to another using a stamp. Specifically, once the sacrificial layer is partly removed, a stamp is used to literally peel-off the NM from the original substrate and transfer it onto the new host. A stamp needs to establish a strong bond with the membrane during pick-up, i.e., greater than the adhesion to the original substrate. It is advantageous to partially underetch a membrane. In this case the unetched portion of the sacrificial layer oxide will support the membrane and cause it to remain flat. Depending on the thickness of the membrane, peeling of growth substrate can generate wrinkles and cracks. The best peeling technique is to pry upward a corner of the substrate to initiate peeling. This technique prevents sharp bending of the stamp and membrane. Once peeling is initiated, the growth substrate can be debonded by holding the substrate with a tweezers and carefully holding the stamp on a flat surface (see Fig. 2.10).

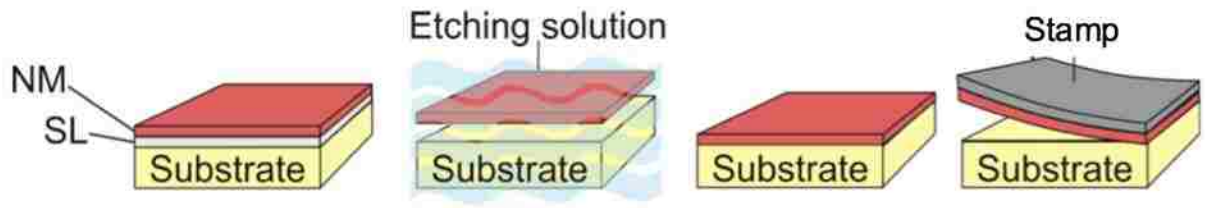

Figure 2.10: Schematic illustration of the release and dry transfer of a NM using a stamp

2.2. Characterization of the effectively compliant layered substrates (ECLS)

This section describes the methods employed to characterize the wettability of the compliant substrates. The technique employed to estimate the elastic moduli of the bare PDMS and the ECLS is also reported here.

2.2.1. Contact angle measurements

Surface wettability is determined by contact angle measurements. The contact angle forms when a liquid meets a solid, as the liquid becomes rounded due to its own surface tension. The contact angle is an angle of straight lines tangent to the outline of the droplet, at the liquid/solid interface or endpoint of the droplet. Hydrophobic surfaces have a contact angle with water greater than 90^{o}. On the other hand, when the contact angle is less than 90^{o}, the surfaces are considered to be hydrophilic (see Fig. 2.11).

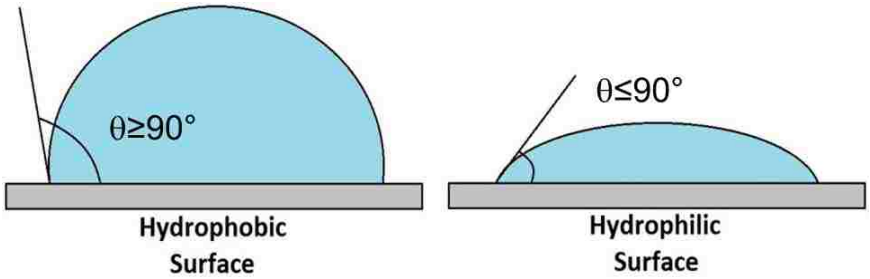

Figure 2.11: Schematic illustration of a hydrophobic surface, $\theta \geq 90°$ (left) and a hydrophilic surface, $\theta \leq 90°$ (right)

Contact angle measurements were performed using a model 100 manual goniometer (Rame-Hart). Briefly, 5.0 µL drops of deionized water were pipetted onto the center of the sample surface. The contact angle between the water droplet and the sample surface was determined using the DROPimage Standard program (ramé-hart). The contact angles were measured after few sec to obtain the static contact angle. Each measurement was taken at least 5 times and the results were averaged out.

2.2.2. Nano indentation/ Atomic-force microscopy (AFM)

Indentation testing is a simple and convenient way to measure the elastic properties of a material. It involves pushing an indenter tip into a material and measuring the load versus displacement curve (see Fig. 2.12). In this study, a TI 950 TriboIndenter (Hysitron, Inc.) and an Atomic Force Microscope (Asylum MFP-3D-BIO^{TM}) are used as nano mechanical testing tool to perform controlled experiments on compliant base substrate and the effectively compliant layered substrates.

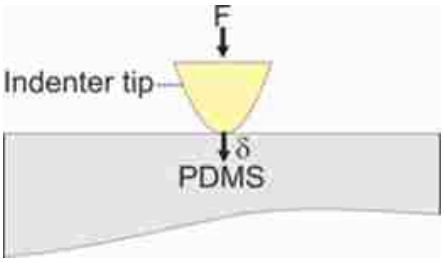

Figure 2.12: Schematic illustration of indentation technique

I use a spherical titanium nitide (TiN) tip with radius 20 nm as an AFM probe for nanoindentation. Initially, to determine spring constant of the probe a sample with known stiffness like glass is used. All samples were indented at a constant force. Five indentations per sample were performed. A schematic representation of a typical data set obtained with indentation is presented in Fig. 2.13. Parameter P defines the load and h is the displacement relative to the initial undeformed surface. The linear range of the unloading curve is analyzed with the Oliver-Pharr method to calculate the elastic modulus of the sample. The Oliver Pharr method uses the plot of applied load, P, and penetration depth, h, to find the slope of material upon unloading, dP/dh. Using slope, I calculated the effective elastic modulus (Eeff) of the material from Equation 2-1. The deformation height (hf) is assumed to be zero for elastic body. Displacement (h) in the equation is replaced with that of max displacement (hmax).

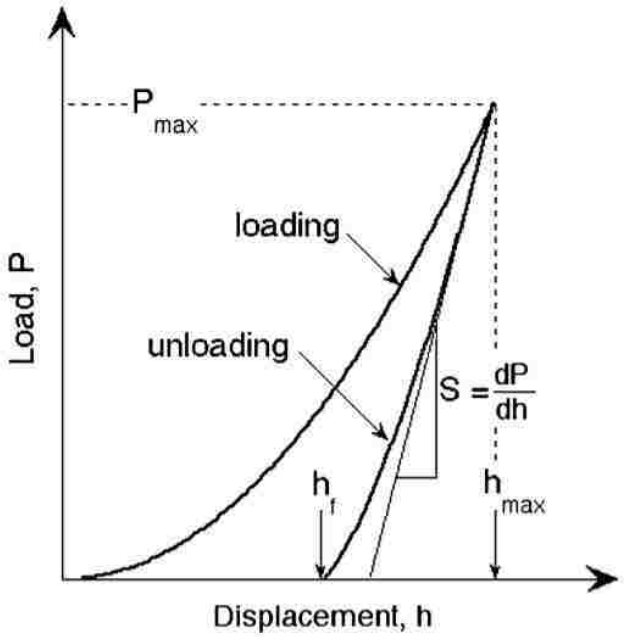

Figure 2.13: Schematic illustration of indentation load–displacement data showing important measured parameters.

$$S = \frac{dP}{dh} = 2\sqrt{R}E_{eff}\left(\mathrm{h} - h_f\right)^{1/2} - (2.1)$$

$$h = h_{max} \;\; \& \;\; h_f = 0 \text{ (Elastic material)}$$

$$\frac{1}{E_{eff}} = \frac{1-\nu^2}{E} + \frac{1-\nu_i^2}{E_i} \qquad - (2.2)$$

The effective elastic modulus (Eeff) includes elastic displacements arising in both the sample material, with a Young's modulus (E) and Poisson's ratio (υ), and the indenter with elastic constants (E_i) and (υ_i). Using equation 2-2, The actual elastic modulus for sample material is determined. Different formulations of PDMS are characterized for elastic modulus using this technique. PDMS is known to exhibit essentially elastic behavior in the deformation range applied in this study. Samples are indent at multiple places to record the homogeneity of the surface. Results for various PDMS formulation are presented in Chapter 3.

2.3. In vitro study: cell culture protocol and cell characterization methods

In this section I report the methods used in *in vitro* study to evaluate response of biological cells on the fabricated substrates. A comparative analysis of cultured cells on various ECLS platforms and reference substrates is conducted through, standard studies like cell viability, cell proliferation, cell cytoskeleton and focal adhesion; characterization techniques like, flow-cytometry, bright-field and confocal fluorescence microscopy are used for this study.

2.3.1. Cell Culture

All chemicals, culture media and reagents used in this cell culture study are purchased from Thermo Fisher Scientific, unless otherwise mentioned.

Cell Type. Mouse extracted 3T3 fibroblast were used in this study. NIH-3T3 fibroblasts are cultured with Hyclone Classic Liquid Media: Mimimum Essentail Medium (MEM) Alpha MEM supplemented with 10% (v/v) fetal bovine serum (Hyclone, Logan, UT), 1% (v/v) penicillin/streptomycin (P/S), and 1% (v/v) fungizone at 37°C and 5.0% carbon dioxide.

Cells Starting. 3T3 fibroblast cells stored in liquid nitrogen and cell culture media and any assays stored in refrigerators are warmed up in a water bath before use. Cell culture workplace has the common requirement of being free from bacteria. The hood is prepared by cleaning off the surface, containers, flasks, and pipettes with 70% ethanol to kill off any residing bacteria before used in a hood. Once 3T3s are defrosted and media is warmed up, 15mL of media is added to cover the surface of 75 cm2 (standard 75T flask) tissue culture polystyrene (TCPS). Defrosted cells are then added to the flask and are left to grow till 80% confluence in an incubator at 37°C with 5% CO_2. Every two days' culture media is replaced by vacuuming off the old media making sure not to scratch cell surface. It is to be noted that, culture medium is one of the most important components of the culture environment, because it provides the necessary nutrients, growth factors and hormones for cell growth, as well as regulating the pH and osmatic pressure of culture.

Cells Splitting Once cells reach confluence of 80% or greater, cells are split into new flasks to further continue growing. Split procedure include, pipetting off media, rinsing cells with 5 mL Dulbecco's phosphate buffered solution (DPBS), then use 2 mL of 0.25% (w/v) trypsin which helps cells to pop off from the surface. 75T flask is then placed in an incubator for ≈ 2-5 mins. After incubation to

separate the cells, rock the flask rigorously. Finally, cells floating in trypsin solution are transferred into two or three new flasks with fresh media.

Cells seeding. Before cell seeding, samples are sterilized for tissue culture use via a 45 minutes long standard autoclave procedure. Once sterilized, samples are loaded into a flat bottom non-tissue culture polystyrene 24 well plates (3370, Corning, Lowell, MA). 24well plate flask has well of size 15 mm diameters each. All samples studied in this thesis are sized to fit the well. 2ml of media is added to each well to cover the samples. Cell seeding follows similar procedure to that of cell splitting up until we have floating cells in trypsin solution. The trypsin solution is then transferred to a micro centrifuge tubes and centrifuged at 2000 rpm for 5 minutes. Trypsin is pipetted off carefully and the pelleted cells are resuspended in 2 mL of fresh culture media. Cell concentration is determined using a hemocytometer (1483, Hausser Scientific, Horsham, PA). Samples are seeded with 20,000cells/well by adding corresponding amount of cell solution to each well. As per experiment, cells are allowed to grow on a particular sample for designated times in an incubator with standard cell culture environment

2.3.2. Cell characterization: *Flow cytometry*

Cell growth and viability were quantified using a flow cytometry study. Briefly, flow cytometry is a laser-based, biophysical technology employed in cell counting, cell sorting, and biomarker detection. Cells are first stained with antibodies and visualized by the excitement of fluorescent antibody labels. Stained cells suspended in a stream of fluid are passed through an electronic detection apparatus, which allows analysis of the physical and chemical characteristics of particle and actively separate and isolate particles having specified properties. The Instruments has multiple lasers and fluorescence detectors allowing for multiple antibodies

labeling, and precisely identifying a target population by their respective markers.

For cell viability and proliferation, four samples of each type are cultured with 3T3s fibroblast cells at 20,000cells/well. Cultured cells on samples are assessed at four time points, i.e., after 12 hrs, 3, 5 and 7 days in vitro (DIV). At each time point, cells are popped off by 0.25% trypsin, the solution is centrifuged; I carefully remove the trypsin leaving the cell pellet at the bottom of the tube. Cell pellet is then resuspended in a 1x annexin binding buffer. Cell proliferation was determined using AlexaFluor 488 Annexin V/Dead cell apoptosis kit (V13241, Life Technologies) according to manufacturer's instructions. All samples are incubated with 100 ul staining solution [5 uL Annexin V and 1 uL propidium iodide @ 100 lg/mL in 1 annexin binding buffer] for 15 min. Samples are read on Accuri C6 flow cytometer (BD Bio.). For all experiments, media is replaced after every two days.

Analysis of flow cytometry data involves displaying the data on a sequence of plots and estimating the percentages of various subpopulations identified from the plot. The method used for this analysis is a progressive reduction of the raw data into subsets using gates. The gated cell population is tested for increased annexin V/Alexafluor 488 and propidium iodine, using quadrant gates. Necrotic controls are achieved by incubating cells with 70% (v/v) ethanol. Apoptotic controls are achieved by leaving cultures at room temperature overnight. An unstained cell gate is established to remove debris.

Optical microscopy

Both inverted and top-down optical microscopes were used to image ECLS microstructure platforms and to perform cell imaging. In tissue culture, during time-lapse imaging, the optical microscope was equipped with a micro-incubator

(Biosciences Tools,CA, USA), so that the temperature was kept at 37C (Also CO_2 (5%) and humidity (95%) were controlled to ensure the appropriate environment for cells.

2.3.3. Cell characterization: *Immunofluorescent staining of cytoskeleton structure*

Cytoskeleton and adhesion mechanisms of the cells on substrate are investigated through Immunofluorescent staining of cytoskeleton structure and imaging using confocal fluorescence microscopy. Immunofluorescent staining makes use of specific antibodies to locate and identify various cell expressions. Primary antibody is intended to bind to a particular element, while a secondary antibody conjugated to a fluorochrome is intended to bind to the primary antibody. Upon absorption of high energy light, the fluorochrome emits light at its own characteristic wavelength (fluorescence) and thus allows detection of complex cell expressions

Staining procedure is as follows, I start with fixing 3T3 fibroblast using 10% formalin for one hour followed by a DPBS wash (2x). Cells are then permeabilized with 0.01% (v/v) Tween20 in DPBS (PSBT) for 15 min followed by reactive ion removal using 10% (m/v) sodium azide and 10 M H2O2 in PBST. Sample were then washed twice with PSBT and placed in Blocking solution (BSA) at room temp incubated for 30 min. Primary antibodies (MT FITC phalloidin, vinculin) diluted 1:75 in a 3% (w/v) BSA solution is stained for 60 min at room temp. Primary antibodies after staining are washed twice with PBST followed by similar staining procedure for secondary antibodies goat anti-mouse AlexaFluor 488 (A11001, Invitrogen) 1:400 dilution in 3% (w/v) BSA solution for 60 min at room temperature, followed by a final wash in PBST(2x). In the end, samples were

mounted using Fluoromount, F4680–25ML on glass slides and sealed with clear nail polish.

Confocal microscopy

The confocal microscopy employed specifically captures the emitted fluorescent light, and allows it to pass through a confocal aperature (pinhole) to reduce the "out of focus" light. Focused light is then passed through emission filters and photo multipliers to generate a very high resolution image of the specimen's internal expressions.

Images of fluorescently labeled cells are performed on an inverted laser scanning confocal microscope (Zeiss LSM 510 META microscope) with oil immersed objectives. Analysis of data involves displaying the data on similar intensities in respect with gain and set point for F-actin fiber organization and focal adhesion staining on different substrates.

Chapter 3. Results: ECLS fabrication and characterizations

In this chapter, I present effectively compliant layered substrates based on silicon nanomembranes and PDMS substrates. This chapter is organized in the following way: in section 3.1 the rationale for ECLS systems in regards with NM for mechanical matching is elaborated. Section 3.2 shows synthesis, modification and systematic selection of compliant base from various formulations of PDMS. Results from characterization of various PDMS for hydrophobicity and mechanical properties are presented. In section 5.3 the fabrication of various ECLS like, large area supported, small area supported, and edge thundered are presented with the help of schematics and optical microscope images. Results from mechanical characterization of ECLS are reported and discussed in this section.

The key aspects that are involved in development of ECLSs are

1) to define the most suitable NM geometry in order to reduce stiffness;

2) to select an ultra-compliant substrate with mechanical and chemical stability;

3) to fabricate ECLS with a good chemical and mechanical stability;

3.1. Rationale for ECLS approach.

Stiffness (k) is an extensive property of an elastic body and it's strongly dependent on 1) the mode of deformation (e.g. stretching, bending, and shear); 2) the elastic modulus and Poisson ratio of the material; 3) the geometry of the elastic body (see Fig. 2).

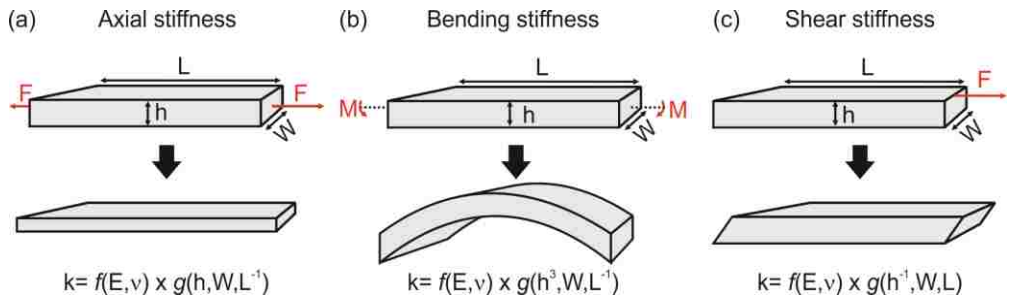

Figure 3.1: Stiffness of a plate with rectangular cross-section (k). The relationship between k, the geometry of the plate and its elastic constants (E, Elastic modulus and, Poisson's ratio) is summarized for three different modes of deformation.

Figure 3.1 schematically illustrates three different modes of deformation of a plate with rectangular cross- section. The dependence of the corresponding stiffness, k, on the elastic properties and the geometry of the materials is also specified. Figure 3.1 (a)-(b) shows that the axial and bending stiffness of the plate scale with its thickness, h, as ~h and ~h3 respectively. For all modes of deformation depicted in Fig. 3.1 stiffness is also defined by the lateral dimensions of the elastic body (L and W in Fig. 3.1 (a)-(c)).

TSP approach, namely, Thin, Shape, and Perforate borrowed from textbook knowledge as descried above is exclusively implemented to tailor stiffness of inorganic semiconductor material. By moving from bulk semiconductors to a nanomembrane, a significant decrease in axial and bending stiffness is observed. Shaping NMs refers to varying in-plane lateral dimensions to further tune stiffness. Additionally, perforation of the NM, which results in an effective decrease of the cross-sectional area, is also used to increase compliance. More importantly, the implementation of TSP approach to tailor the geometry of the NM can be easily done by using well-established top-down processing techniques. Fig 3.2 summarizes the TSP approach.

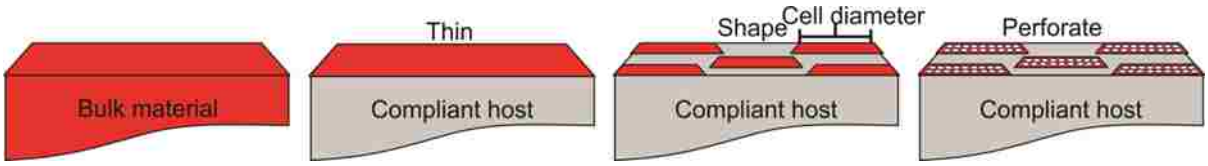

Figure 3.2 Proposed approach to tune the stiffness of the ECLS. From left to right, bulk materials are made into NMs and transferred to a compliant host. (NMs are exceptionally compliant to bending and axial deformation due to their nanoscale thickness). In addition, NMs are patterned into lateral dimensions matching the diameter of biological cells and perforated to further reduce their stiffness.

The rationale for current study for the most part is derived from a recent work, in which finite-element modeling (FEM) was employed to investigate the effective mechanical response of ECLS to contact loading. The study demonstrated that the effective stiffness of a single-crystal (high-modulus) semiconductor sheet on a low-modulus substrate, with a high mismatch in their elastic moduli ($>10^5$), is defined by the elastic moduli of the constitutive materials, the thickness of the sheet, and by the extent of the loaded area. In addition, a key relationship was established between material properties and probe dimensions (i.e., indenter radii) that define the load deformation response and effective stiffness.

Simulations performed with indenters of various sizes have shown that the response of SiNMs on compliant substrates approaches that of the bare substrate when the indenter radius is larger than tens of micrometers. Typical diameters of biological cells are ~ 100s of micron. Figure 3.3 (Reprinted from F. Cavallo, D. S. Grierson, K. T. Turner, and M. G. Lagally, ACS Nano, 5, 5400 (2011)) shows that for such a contact radius matching the lateral dimensions of biological cells the mechanical response of thin semiconductor films on compliant hosts is determined by that of the host. As stated earlier, the other major drive in current work is the availability of techniques to harness intrinsically stiff, electrically and optically active function material like silicon, in the form of large-area, thin (5 - 100 nm)

membranes. Fusion of these two ideas suggested that appropriate selection of the compliant host and NM geometry allows creating inorganic device graded platforms with stiffness matching the one of a typical cellular environment.

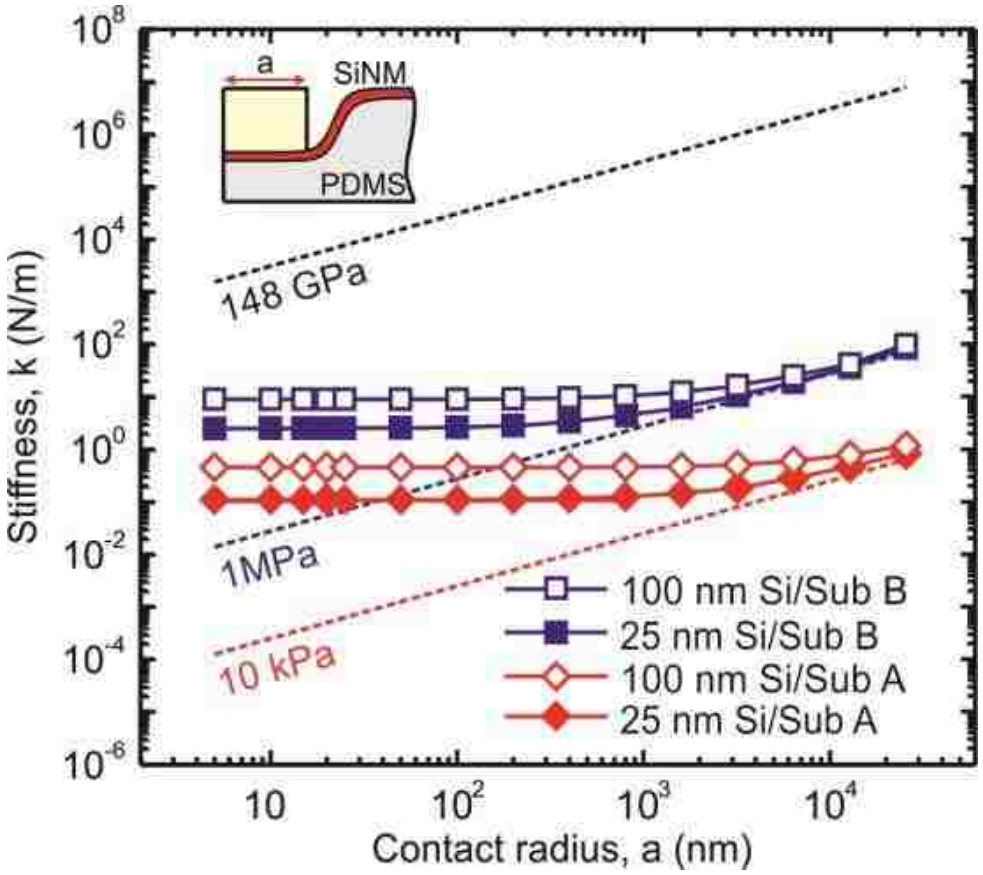

Figure 3.3: Effective stiffness vs. contact radius as determined by FEA for a rigid, cylindrical flat punch indenting into three bulk materials with elastic modulus of 10 kPa (Substrate A, red dashed line corresponding roughly to PAAG), 1 MPa (Substrate B, blue dashed line, corresponding roughly to PDMS), 148 GPa (black dashed line, corresponding to bulk Si); 25 nm and 100nm SiNMs on substrate A (red solid diamonds and red open diamonds, respectively); and 25 nm and 100nm SiNMs on substrate B (blue solid squares and blue open squares, respectively). The contact radius, *a*, is the radius of the cylindrical indenter, and the SiNM is assumed to be perfectly bonded to the PDMS substrate. **Reprinted from F. Cavallo, D. S. Grierson, K. T. Turner, and M. G. Lagally, ACS Nano, 5, 5400 (2011)**

3.2. Compliant substrates with tunable mechanical properties:

In this study, the goal is to have a compliant substrate with elastic modulus tunable between ~0.001 and 1 MPa to match the wide range of elastic properties of biological tissues. In principle, compliant base substrate for ECLS can be any of the various commercially available elastomers, such as poly(methylmethacrylate) (PMMA), polyvinylchloride (PVC), polycarbonate (PC), polystyrene, polyurethane, and poly(dimethylsiloxane) (PDMS) and etc.

I have chosen poly(dimethylsiloxane) (PDMS) as our base substrate, because PDMS is inexpensive, easy to fabricate, biologically inert, and optically transparent, allowing for both optical and fluorescent microscopies. In addition, PDMS is nontoxic, autoclavable and does not swell or dissolve in culture medium. For all the reasons listed above, PDMS is widely used as cell culture substrate in *in vitro* studies. An additional value is that PDMS elastic modulus can be controlled in a wide range (~kPa-10s MPa) independently of other materials properties, the tunable stiffness range from values matching brain-tissue to bones.

As detailed in chapter 2, PDMS is an assembled network of polymer chains which cross-linked to a certain degree, depending on its composition and fabrication process. Briefly, commonly used PDMS (Sylgard 184) constitute of a two-part kit, the base and the curing agent. The kit is to be mixed prior to use and to be cured at a given temperature/time. In general, the ratio between the curing agent to base defines the degree of cross-linking and the elastic modulus of the material. The higher ratios between base and curing agent yield materials with lower elastic moduli, due to a lower degree of cross-linking in the polymer network. However, having higher ratios i.e. lesser degree of crosslinking leads in free polymer chains

which can leach out over time, thereby creating a toxic environment for biological cells. In this thesis, instead of just a Sylgard 184 kit, I have used Sylgard 184 in conjuncture with commercially available elastomer namely Sylgard 527. It is reported elsewhere, that having a blend of 527 and 184 allows us to fabricate PDMS in ranges of kPa without any problem of free polymer chains. To attain lower elastic modulus instead of increasing the ratio between the base and curing agent, here I increase the ratio between two PDMS kits,

Figure 3.4 shows, Sylgard 184 and Sylgard 527 made as per manufacturer's direction in their standard form i.e. Sylgard 184 in 1part curing agent to 10part base, and Sylgard 527 in 1:1 ratio of PartA and PartB, which allows them to maintain their stoichiometric stability. Accordingly, we see a standard PDMS made out of 184 to be a very rigid rubber-like substrate, and on the other hand standard Sylgard 527 is more like a semi-liquid gel. For a successful ECLS fabrication the goal is to find a chemically and mechanically stable compliant substrate. Chemical stability is essential to avoid any toxic behavior which may influence bioactivity of ECLS in tissue culture. Inadequate mechanical stability of compliant substrate would cause handling issues during ECLS fabrication process. Moreover, the objective is to seamlessly vary elastic modulus in wide range without change in material properties. To do so, various mass-to-mass ratios between the two kits are varied to tune stiffness of PDMS without any major change in chemical and mechanical stability. The different formulations of mass ratios investigated in this thesis are reported in Table 3.1.

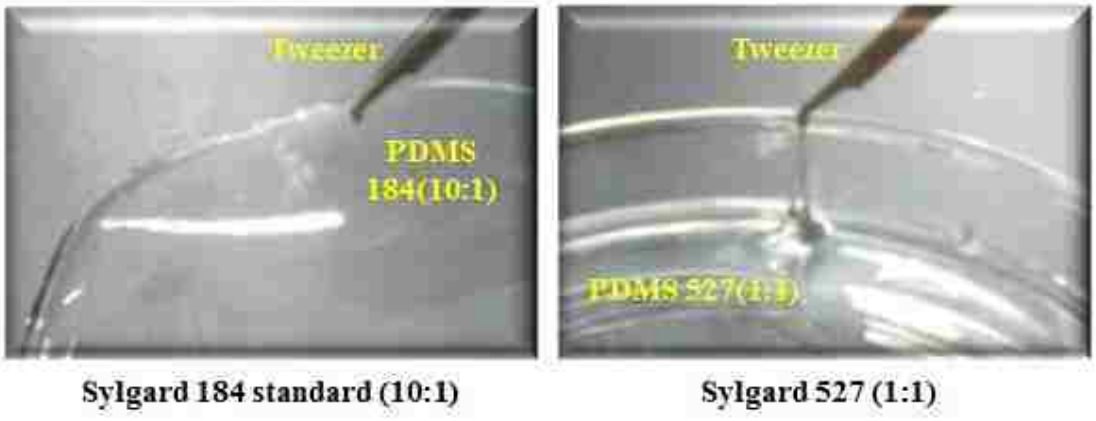

Figure 3.4: photographs show a standard 184 (10:1) PDMS and pure 527 (1:1) fabricated as per manufacture direction, holding by a tweezer

184: 527 184 (Base: Curing agent): 527 (Part A : Part B)
1:0 (10:1) : (0:0)
1:10 (10:1) : (1:1)
1:20 (10:1) : (1:1)
0:1 (0:0) : (1:1)

Table 3.1: Formulations of different PDMS investigated in this study

1. PDMS 184(10:1) is a standard PDMS with both chemical and mechanical stability. It is easy to handle and can seamlessly translate into ECLS. Elastic modulus of PDMS 184(10:1) is reported to be in the range of Mpa. In this study, as proposed ECLS are specifically aimed at soft cell such as neuronal cell, brain cells and etc. Elastic modulus in range of Mpa is considered to be relatively hard. On the other hand, if ECLS are fabricated for a bone-like cell which prefers a hard substrate, PDMS 184(10:1) is an ideal base substrate for a

Hard ECLS. Nevertheless, for the most part of the study, I use PDMS 184(10:1) as a bench mark for chemical and mechanical stability for low-elastic gels.

2. PDMS 184(50:1) is a variation of standard PDMS 184 (10:1), it is fabricated by lowering the crosslinking agent. Here I have reduced PDMS to 50 part of base to curing agent. It is reported to have elastic modulus in the range of 10's of kPa. The reduced elastic modulus in this case is ideal for fabrication of a soft ECLS platform. Nonetheless, it is argued in the literature that, uncrosslinked chain can leach out in culture media making it toxic, thus undesirable for cell study. Moreover, PDMS (50:1) was difficult to handle, extremely adhesive because of open chains on surface and very gel-like, which makes it problematic to translate into an ECLS.

3. PDMS hybrid 184:527(1:10) is a blend of 527 (1:1) and 184 (10:1) in 10part to 1part. Here, I am able to maintain stoichiometry of PDMS 184, by fabricated in its standard ratio, and addition of PDMS 527 kit lower the elastic modulus of the combined blend. Both pure 527 and pure 184 are independently made and blended into 10:1 ratio, which yields a PDMS without leasing out chains. Elastic modulus of hybrid PDMS (1:10) is reported to be in range of 50's of kPa. It is exceptionally stable, easy to handle, and can easy be translate into ECLS.

4. PDMS hybrid 527:184 (1:20) formulation is a blend of 527 (1:1) and 184 (10:1) in 20parts to 1part. It is fabricated similar to that of hybrid (1:10) instead in 1:20 ratio. The elastic modulus for this formulation is not reported, I expect it to be in range of 10kPa. Hybrid (1:20) is significantly stable, easy to handle, and easy to fabricate ECLS.

5. PDMS hybrid 527:184 (1:0) is a pure 527 (1:1) ratio. The pure 527 is a complete gel, claimed to have elastic modulus in the range of 5Kpa. The PDMS didn't polymerize, it is a pure semi-liquid gel and fabricating of ECLS out of it is extremely difficult.

For further processing in ECLS fabrication and *In Vito* cell culture study, I have used Hybrid (1:10) and Hybrid (1:20) PDMS as my compliant base substrate based on their chemical and mechanical stability with elastic modulus in ranges of kPa.

3.2.1. Elastic modulus of different PDMS formulation

The elastic moduli of the different formulations of PDMS discussed above are measured via nanoindentation technique using an atomic force microscope. A representative force vs displacement plot generated by indenting standard PDMS 184(10:1) using a TiN coated AFM probe of tip radius 20nm is shown in figure 3.5. The figure displays a red loading curve, a blue unloading curve and a bouncy retraction of tip at the end which is due to adhesiveness of polymer. I approximate stiffness(S) of the substrate by measuring the slope of linear region in unloading curve. Elastic modulus is calculated using standard Oliver-Pharr method defined for elastic bodies. 5 indentations are done on each sample. Details on indentation procedure and analysis using Oliver-Pharr method are described in Ch. 2. The measured elastic moduli for each formulation are presented in Table 3.2.

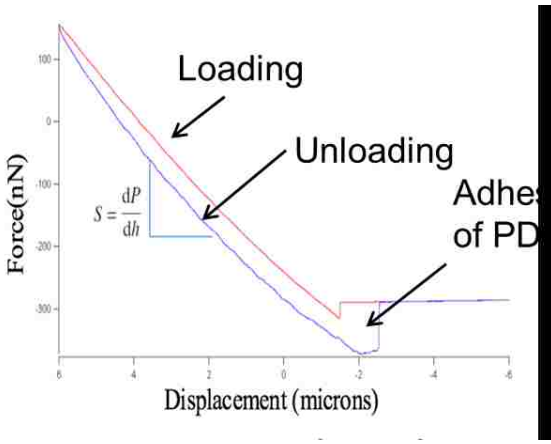

PDMS 184:527	Elastic modulus
Standard (10:1) : (0:0)	1.87 ± 0.13 MPa
1:10 (10:1) : (1:1)	138 ± 3.83 kPa
1:20 (10:1) : (1:1)	78 ± 0.83 kPa

Figure 3.5: shows Force vs displacement plot for a 184(10:1) PDMS; Red curve indicates loading of AFM tip into PDMS; Blue curve indicates unloading of tip from the substrate. Bouncy retraction of tip from substrate indicated adhesiveness of PDMS.

Table 3.2: Elastic modulus of various Formulations PDMS investigated in this study

Elastic modulus decreased from 1.87± 0.13 MPa to 78± 0.83 kPa, as expected with increase in mass ratio of Sylgard 527 relative to Sylgard 184. Evaluation by nanoindentation displayed discrepancy in elastic modulus for what is reported. Hybrid (1:10) - 184(10:1) and 527(1:1) is reported to have elastic modulus of 50kPa; however, I measure it to be approx. 140.2 kPa. I assume the variance in measurement is due to the difference in technique used, as reference measures elastic modulus using a tensile tester and I expect measurements of AFM used in this study to be localized then that of a tensile tester. Unreported Hybrid (1:20) - 184(10:1) and 527(1:1) is measured to be approx. 80kPa. Differences between formulations are found to be significant and the standard deviation of elastic modulus of samples is found to be within the signal noise and displayed as zero.

Further in this thesis, to fabricate various ECLS platforms and access biological cells to study mechanical response on fabricated substrate (dedicate cht.4). I have used hybrid (1:10) -184(10:1)/527(1:1) and hybrid (1:20) -184(10:1)/527(10:1), because of their respective elastic modulus and mechanical/chemical stability.

3.2.2. Modified PDMS

The biocompatibility of a material is determined by its chemical structure, surface property and surface chemistry, which includes surface functional group, surface charge, and hydrophilicity/hydrophobicity. PDMS intrinsically is very hydrophobic in nature, and when diluted to reach lower elastic modulus, it is also observed to be highly adhesive, which results in difficult handling and low yield during fabrication of the ECLS.

Accelerated solvent extraction (ASE) n-hexane/acetone (1:1v/v) is used as a cleaning method to reduce adhesive nature of low-elastic modulus PDMS formulations in this study. The solvent mixture helps in release of small polymers from silicone rubber called oligomers, which are potentially causing PDMS to be adhesive in nature and any loose oligomers leashing out in culture media might also lead in toxic behavior. An optimized time and temperature (Temp 120-130 for 6-12hrs) was selected to extraction oligomers with highest release rate. The step by step procedure to undertake cleaning process is presented in Chapter 2.

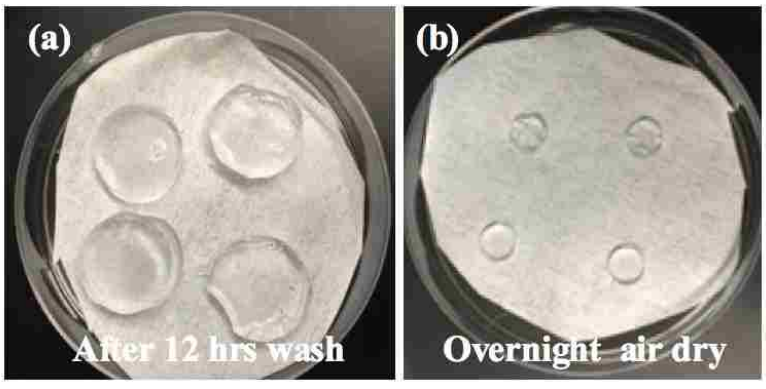

Figure 3.6: Hybrid 1:20 PDMS (12mm dimeter) undergoing accelerated solvent extraction for 3hrs a) swollen PDMS (left) immediately after treatment, b) samples overnight air dried in fume hood to allow solvent evaporation(right).

PDMS are extremely swollen and fragile after solvent extraction. Swelling in PDMS is due to solvent absorption which results in expansion of polymer chains. Before any further use swollen PDMS gel are air dried in a fume hood to evaporate absorbed solvent. The mass of PDMS, decrease by a fraction as uncured elements are extracted.

Any change in the wettability of the PDMS substrates after solvent extraction is estimated by contact angle measurements (see Ch. 2 for a more detailed explanation of the method). The contact angle measured for PDMS before ASE range from 115 to 130 º. No significant statistical differences observed after solvent extraction for all PDMS formulations investigated.

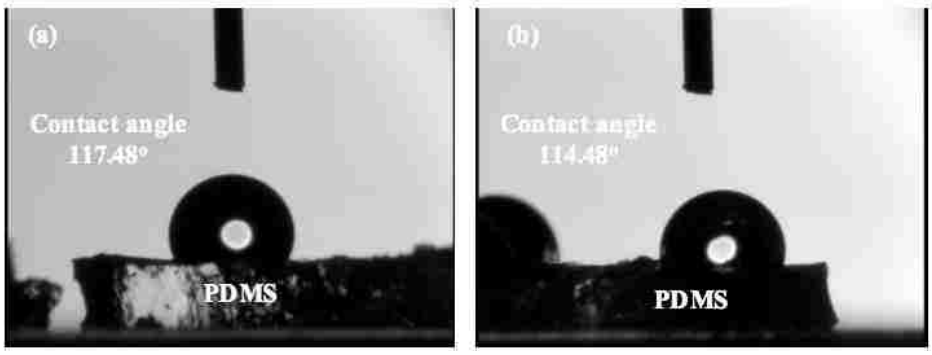

Figure 3.7: a) Contact angle before solvent extraction on hybrid (1:20), b) Contact angle after solvent extraction.

In this study, Ultra Violet Ozone treatment (UVO) is employed to increase wettability of the substrate, as specified in Ch. 2. UVO exposure has shown to follow an inverse proportionality with contact angle as captured in Figure 3.8.

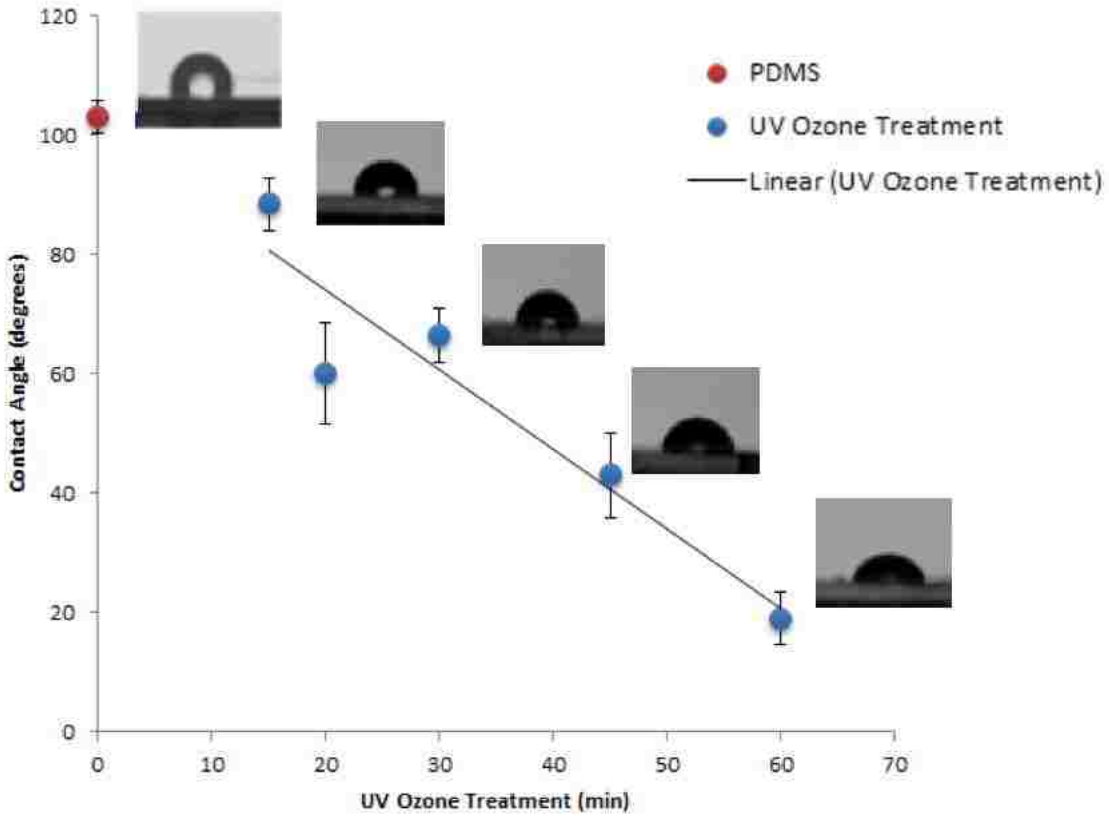

Figure 3.8: UV ozone treatment: exposure time vs hydrophilicity.

PDMS are tested for immediate wettability after fabrication and immediately after UVO treatment. PDMS are stored in water to avoid any hydrophobic recovery; I have examined the wettability of stored PDMS after 48 hrs time point, to see if any hydrophobic recovery happens. Results for different formulation of PDMS are summarized in Figure 3.9.

PDMS Type 184:527 (Part A: Part B): (Base curing : agent	UV-Ozone treatment (Wettability)		
	Untreated (Avg. ^{O}C)	0 hours (Avg. ^{O}C)	48 hrs. in water (Avg.)
1:0 (10:1) : (0:0)	123 ± 5	54 ± 6	56 ± 5
1:0 (50:1) : (0:0)	121 ± 3	61 ± 2	58 ± 7
1:10 (10:1) : (1:1)	118 ± 4	56 ± 8	54 ± 4
1:20 (10:1) : (1:1)	119 ± 2	54 ± 5	56 ± 6

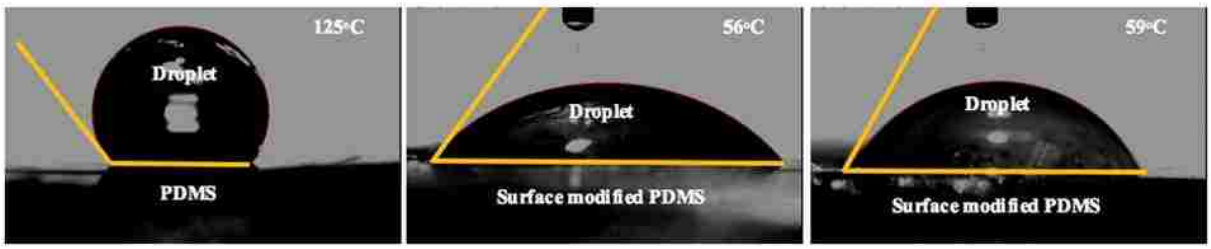

Figure 3.9: Hydrophobic recovery test a) Contact angle before UV-ozone treatment on hybrid (20:1), b) Contact angle immediately after UVO treatment, c) Contact angle after 48hrs in water.

PDMS do not under go any hydrophobic recovery. Wettability test was conducted on all formulation of PDMS stored in water. It is seen that PDMS contact angle measured immediately after UVO treatment remained same after long period of

storage in water. By this point, I have a hydrophilic PDMS, with improved biocompatibility ready for further processing.

3.3. Various ECLS platforms fabricated

In this section, I describe a variety of planar ECLS platforms fabricated as part of the study. ECLS simply put are, NMs transferred on to soft substrate (see figure). Various fabricated planar ECLS include large-area supported NMs on compliant substrate, small area –pixel NM on compliant substrate, and edge-tethered NMs, which are partly suspended over the compliant substrate. To realize each ECLS, I have exclusively used dry transfer technique (detailed in Ch. 2). Schematic and optical micrographs are used to illustrate ECLS in this section.

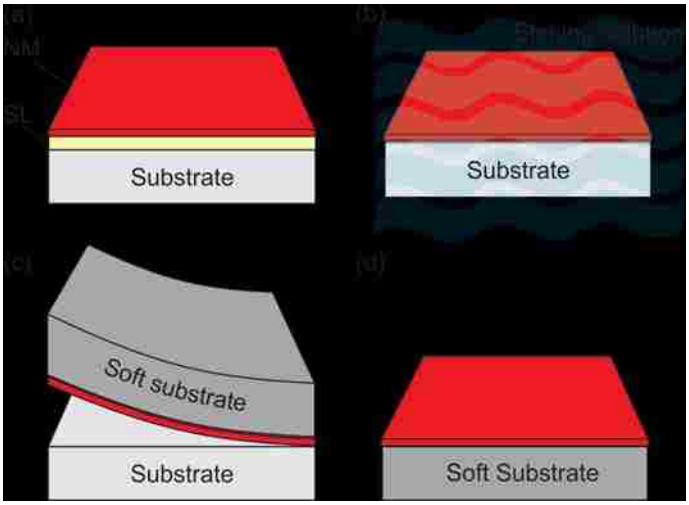

Figure 3.10: Schematic illustration of ECLS fabrication.

Generally, a dry transfer technique employs adhesive stamp to facilitate NM transfer from growth substrate to a new host substrate. Luckily, PDMS, the compliant base substrate that I wish to bond my active functional layer to, is one of the most effective stamps commonly used for dry transfer. PDMS surface energy is just enough to establish a strong bond with the membrane during pick-up.

Different types of ECLS are fabricated in this study to achieve varying mechanical properties by a combination of different configurations of NM and various blends of PDMS as ECLS. NM configurations implemented are derived from TSP approach (detailed in section 3.1) TSP stand for, thinning, shaping and perforation. Here, a large area supported configuration shown in figure is essentially a 1 cm^2 x1 cm^2 lateral size NM with perforation of 5µm holes spaced 60µm apart, transferred on a hybrid (1:20) -184(10:1)/527(1:1). Similarly, a small area supported ECLS is an array of pixel (size: 100µm) transformed on a compliant base. Very minimal to no change in approach is needed to outline different shapes of membranes on Si-layer by optical lithography and RIE etch. However, at release stage geometry and size of NM, i.e. access area provided for the etchant, matters the most. (Detail on release process is specified in Ch. 3).

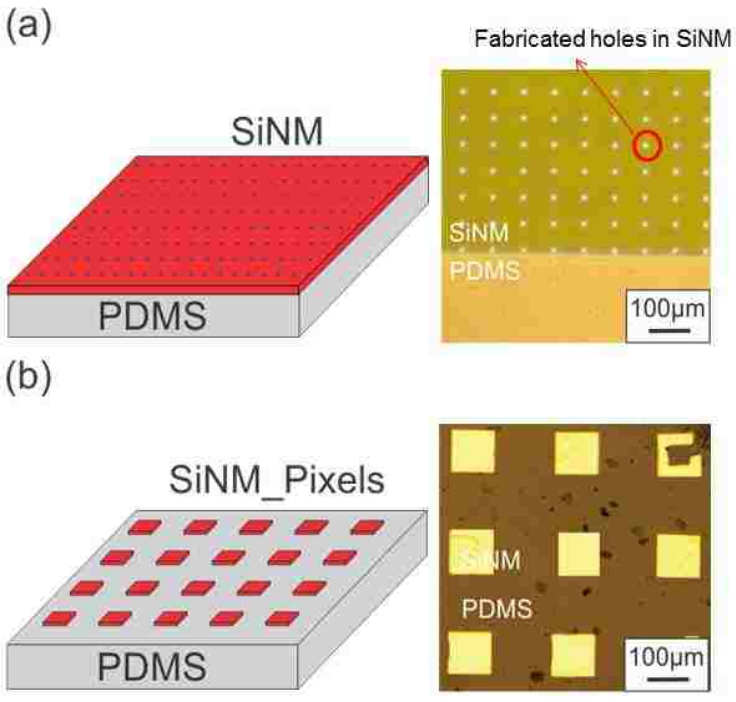

Figure 3.11: Illustrates schematic and optical microscopic images of a) Large area supported ECLS (i.e. 1 cm^2 x1 cm^2 SiNM 220nm on hybrid PDMS (1:10), b) Small area supported ECLS (3x3 array of SiNM 220nm pixel of size 100µm on PDMS (1:10)).

As mentioned earlier, edge-tethered membranes are partly suspended NM on a compliant substrate. It is fabricated through a two-step patterning technique. Firstly, in a conventional way a large area membrane with perforation is fabricated. After RIE etch and PR removal, the sample undergoes a second step lithography to define a suspension pattern. Here I have patterned a suspension of 2mm x 2mm (See figure 3.13) and an array of 100μm pixel (See figure 3.13). Once suspension is defined using lithography, the pattern is selectively etched on to the membrane till a desired thickness using RIE (Etch rate and RIE recipe included in Cht2). Figure shows SINM of 220nm with suspension region of thickness 40nm for both large area suspension (2mm x 2mm) and pixel (100μm). Schematic illustration of edge tethered ECLS fabrication process is shown in figure 3.11. Edge tethered ECLS is realized in final step of peeling SiNM from growth substrate. Result of suspension in an edge tethered membrane on PDMS is shown in figure 3.11.

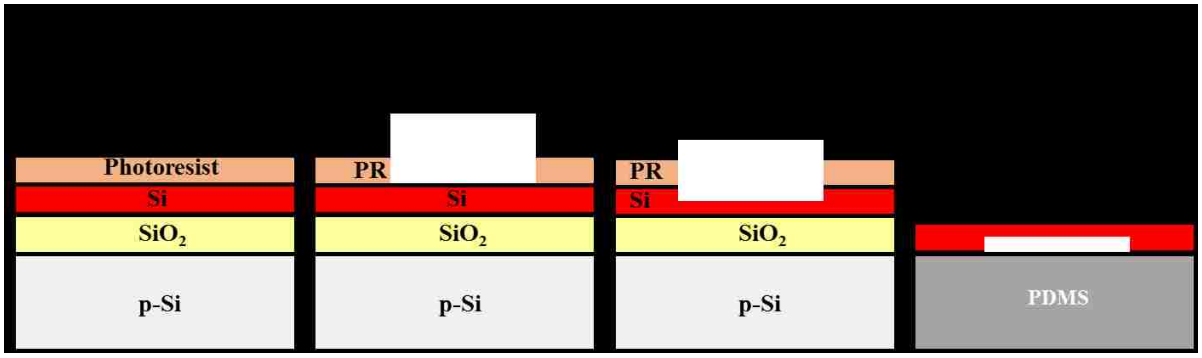

Figure 3.11: Schematic illustration of edge tethered ECLS fabrication process.

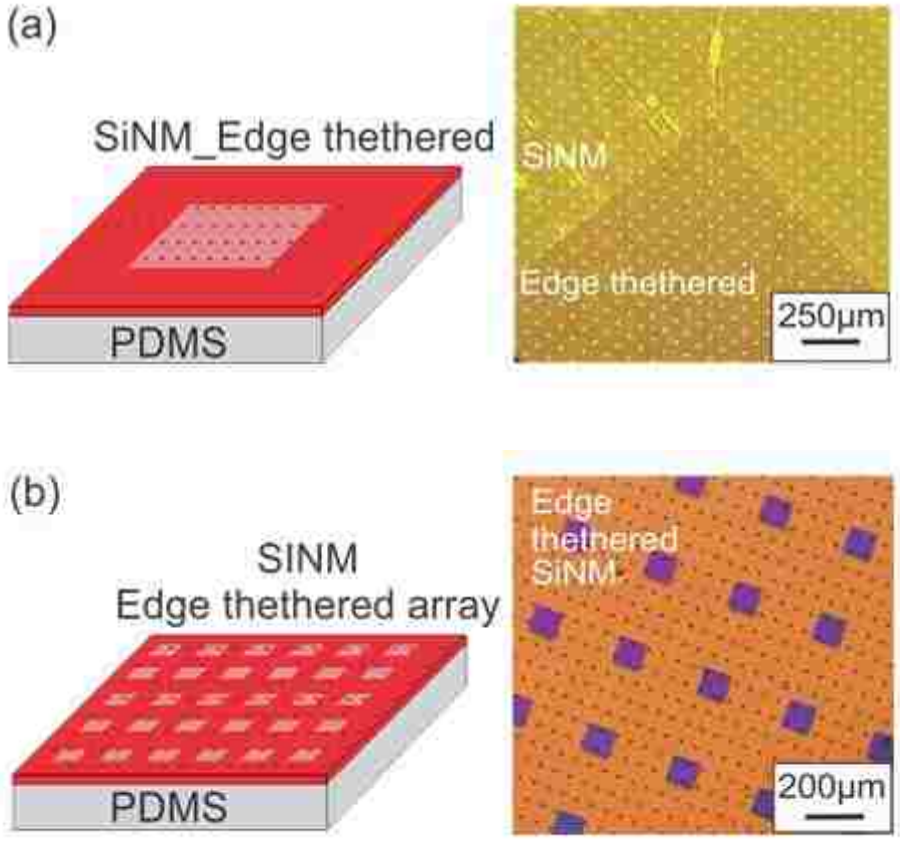

Figure 3.13: Illustrates schematic and optical microscopic images of a) Large – area edge tethered ECLS, SiNM 220nm (1cm x 1cm) on standard PDMS (10:1) with 2mm x2mm suspension of 20nm. b) Edge tethered with 100um suspension of 20nm array on standard PDMS (10:1).

Lastly, figure 3.14 shows, NM with failed transfers (wrinkle and cracks) due to lack of flatness of membranes during pick-up, improper initial contact, NM with thickness < 100nm, extremely soft PDMS and also impatient peeling of growth substrate. All the above mentioned problems and respective solution are explained in detail in chapter 2.

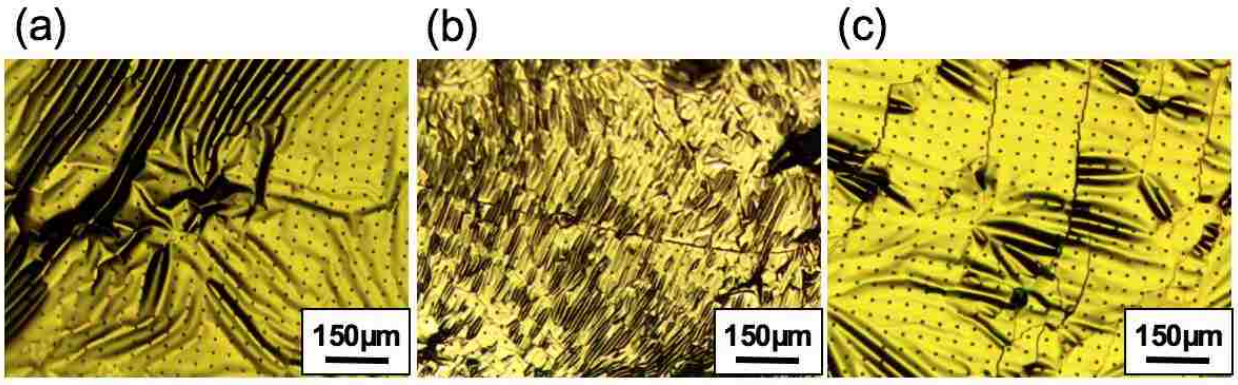

Figure 3.14: (a) shows an image of 220 nm failed transfer causing wrinkle (b) 20nm SiNM failed transferred with lots of wrinkle, due to lesser thickness (c) cracks and delamination of 220 nm NM on a PDMS(<100kPa))

3.3.1. Elastic modulus of ECLS

The effective elastic modulus of the ECLS was characterized by a commercial nanoindentation; specifics are included in chapter 2. The near surface mechanical properties of ECLS platforms consisting of a 220 nm SiNM with 600µm x800µm lateral dimensions patterned in checkerboard fashion, with silicon islands of size 80µm x 50µm, transferred onto two different PDMS substrates namely, a hybrid (1:10) -184:527, a blend of 527 (1:1) and 184 (10:1), with elastic modulus approx. 150kpa, and a standard 184(1:10) 10part base to 1part curing agent, with elastic modulus of approx. 2Mpa. SiNM/PDMSs are indented using a displacement controlled quasi static indent to 1500 nm using a conospherical probe with a 5µm tip radius. 15 indentations are done on each sample. Table 3.3 shows the measured mechanical properties for each sample at comparable depths.

	SiNM 220nm on hybrid PDMS (1:10)	SiNM on standard (10:1) PDMS
Contact Depth (nm)	1138 ± 172	835 ± 53
Storage Modulus (MPa)	0.372 ± 0.019	3.835 ± 0.285
Stiffness (N/m)	2.35 ± 0.17	21.2 ± 1.7

Table 3.3: Near surface mechanical properties of ECLS samples from low load indentation with a conospherical probe with a 5μm tip radius

Storage modulus of SINM (220nm) on hybrid (1:10) measured approx. 372 kPa, and SINM (220nm) on standard (10:1) measured approx. 3.8MPa. SiNM 220nm is expected to be stiff, the two order of magnitude difference in elastic properties of ECLS compared to that of its base can be attributed to the thickness of SiNM. The experimental results fall in agreement with theoretical postulates. Furthermore, this result clearly shows that by tuning in base material from a hard PDMS to a soft PDMS, we see a seamless translation of effective elastic modulus in ECLS structure. One need to acknowledge the fact that, silicon material with ECLS approach has able to change its intrinsic mechanical property in two orders of magnitude compared to that of Bulk silicon (140GPa).

Additionally, to determine the relevance of indentation depth with storage modulus, a probe with 50μm tip radius is indent with a controlled force. 15 indentations are done on each sample. It was observed that with increase in indent depth effective elastic modulus of ECLS decreased. This result highlights the impact of base substrate's elastic properties in determining effective elastic modulus of hard skin – soft base bilayer system (Shown in figure 3.15).

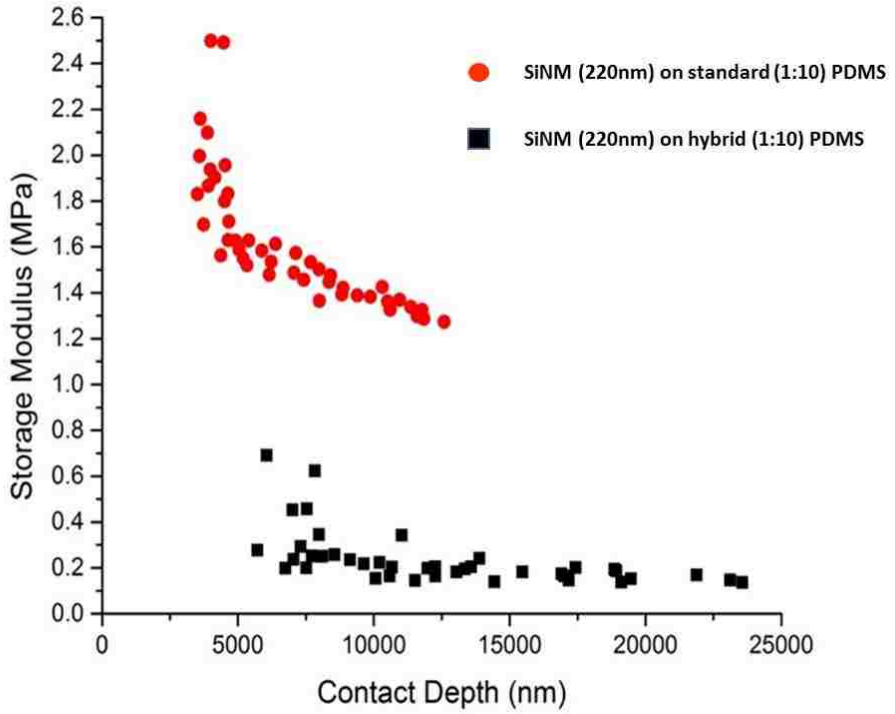

Figure 3.15: Storage modulus with respect to contact depth on 220nm SiNM on standard (10:1) PDMS and 220nm SiNM on Hybrid (1:10) PDMS with a conospherical probe with a 50μm tip radius

Also, as second part of the tests, two ECLS with SiNM of lateral dimension 1cm2 x 1cm2 of two different thickness, specifically SiNM 220nm and SiNM 40nm transferred onto compliant hybrid (1:10) PDMS were indented using a nano-indenters. A flat Al probe with 2mm tip radius was indent with controlled force similar to as stated earlier. Figure 3.16 shows an overlap of loading and unloading curve of a force vs displacement plot of dissimilar ECLSs and bare PDMS to compare slope i.e. the change in stiffness, it is observed that SiNM with thickness in 10's of nm manages to replicate the slope i.e. stiffness of compliant base fluently, compared to that of a 220nm SiNM on same base.

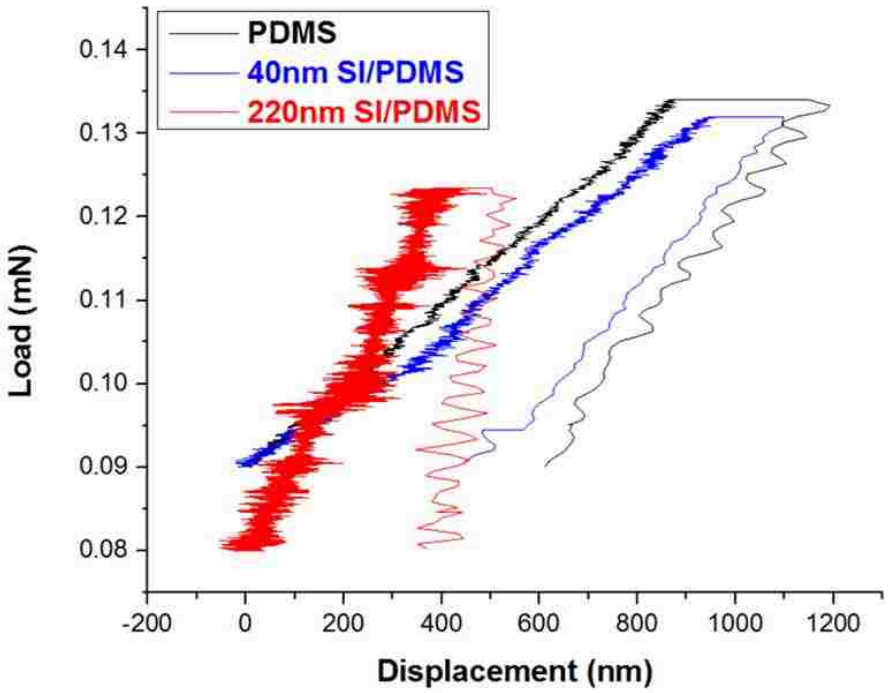

Figure 3.16: Overlap of load vs displacement curve of PDMS; 40nm SiNM on PDMS and 220nm SiNM on PDMS.

In summary, by moving from bulk semiconductors to NMs the stiffness of single-crystalline silicon is reduced by at least three orders of magnitude, and in addition if we compose an ECLS with an ultra-compliant base and an extremely thin silicon film in 10's of nanometer range, we have an ECLS with elastic properties matching to that of their base substrate. By way of explanation, effective elastic properties of ECLS are defined by the elastic moduli of the constitutive materials and the thickness of the top sheet.

Chapter 4: *In vitro* study of cell response on effectively compliant layered substrates

In this chapter I access a well characterized *in vitro* model, such as 3T3 fibroblasts to evaluate cell response on effectively compliant layered substrates (ECLS). Specifically, I used flow-cytometry to investigate cell viability and cell proliferation on Si-based ECLS, as well as on bulk Si and bare PDMS. Proliferation results presented here focus on evaluating acceptance of ECLS in tissue culture, and are used to estimate the impact of substrate rigidity on cell growth; In addition, fluorescence microscopy is employed to capture change in cellular properties attributed to substrate mechanics, such as shape, spreading, and adhesion mechanisms.

4.1. 3T3 Fibroblasts

To study cells on fabricated substrates, I have selected 3T3 cell line which is a standard non-human fibroblast cell line extracted from primary mouse embryonic fibroblast. 3T3 cells are very stable, easy to clone and maintain *in vitro*.3T3s can be bipolar or multipolar and have elongated shapes. I have used these cell lines primarily because 3T3s are well-characterized for studies related to mechanical response of cells on substrates. Previous studies have concluded that 3T3 fibroblasts exercises an increase in proliferation; spreading behavior and exhibits more features of stress fibers and large focal adhesion at increasing substrate stiffness. Figure 4.1: shown a typical 3T3 change in shape and size due to substrates elastic modulus.

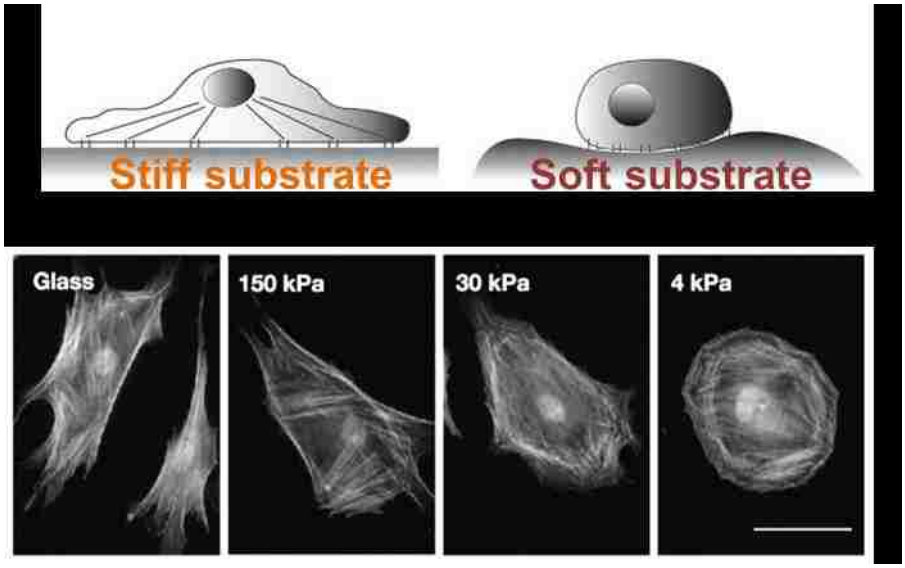

Figure 4.1: Typical 3T3 change in shape and size due to substrates elastic modulus

Adhesion mechanisms especially the focal adhesion points of 3T3 fibroblast on stiff and soft substrates are shown in figure 4.2.

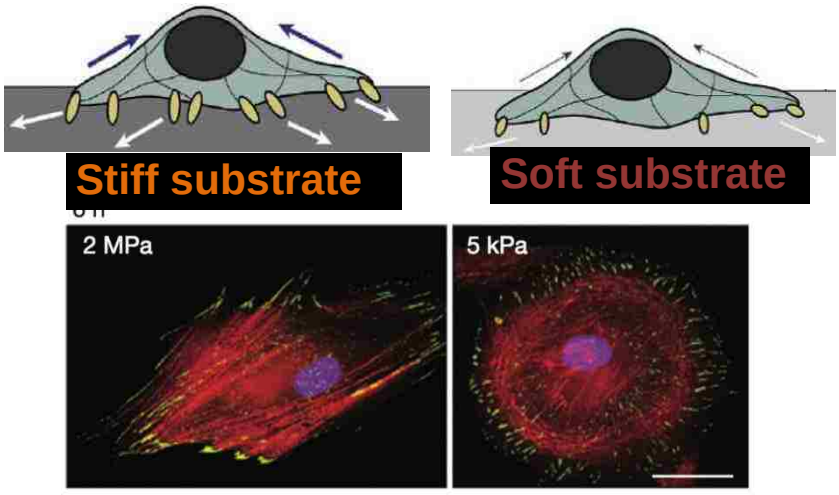

Figure 4.2: Typical 3T3 fibroblast focal adhesion points on a soft and hard substrate

Factor	Response
Spread area	Decrease
Focal adhesion formation	Decrease
Stress fiber formation	Decrease
Apoptosis	Increase
Proliferation (cell growth)	Decrease
Migration speed	Increase
Traction forces	Decrease

Table 4.1: Summary of various response of 3t3 fibroblast to substrate with decreasing elastic modulus

Several groups noted cell growth and apoptosis are also influenced by substrate rigidity. Cells on softer gels maintained a 30–35% apoptosis rate compared to less than 5% on stiffer gels. Thus, increases in cell numbers on substrates of higher elastic moduli can be attributed to both increased cell proliferation and decreased apoptosis. Fibroblast responses to changes in substrate rigidity are summarized in Table 4.1.

4.2. *In vitro* study

3T3 fibroblasts are cultured *In vitro* on four types of substrates, namely tissue-culture polystyrene (TCPS), bulk silicon, bare PDMS, and ECLS. A detailed description of the samples structures used in the vitro study is reported in Table 4.2.

Substrate	Tissue culture Poly-sterene (TCPS)	PDMS 184:527 1:10	PDMS 184:527 1:20	Bulk Si	PDMS 184:527 1:10		PDMS 184:527 1:20	
Skin	None	None		None	40 nm SiNM	220 nm SiNM	<20 nm SiNM	220 nm SiNM

Table 4.2: Summary of all the substrate used for In vitro study

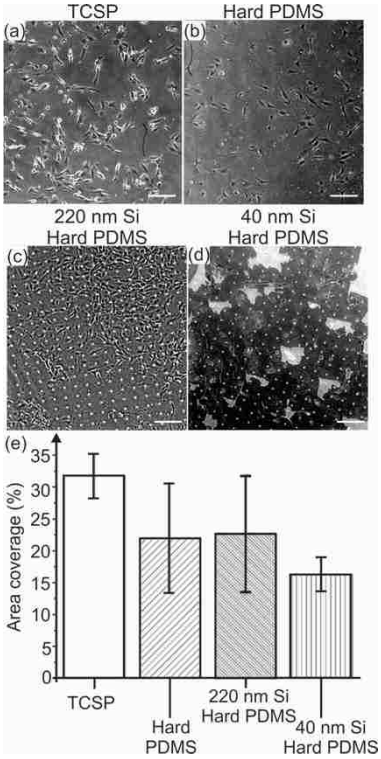

The samples structures specifically TCPS and bulk silicon serve the purpose as reference rigid culture substrate for cell response, whereas bare PDMS serves as a soft substrate with elastic modulus in the range of kPa.

In a preliminary study, ECLS consisting of hybrid PDMS (1:10) and SiNM of thickness 220nm and 40nm were studied using optical microscopy for 12hour time point to access cell attachment and over 7days to access cell proliferation shown in figure 4.3.

bottom-up bright field images of 3T3 fibroblasts cultured on TCPS, hard PDMS and ECLS, namely 220 nm Si/hybrid PDMS (1:10) and 40 nm Si/hybrid PDMS (1:10). Images were taken 12 hours after seeding, seeded at a density of ~18,000 cells/well. No data are available for bulk Si due to the lack of transparency of this substrate in the visible range. This highlights one more advantage of using ECLS, namely the possibility of interfacing cells with a device grade semiconductor, and still being able to assess cell status via bottom-up bright filed microscopy. All this is enabled by the extreme thinness of Si NM, which allows electromagnetic radiation to be transmitted through the film. Imaging and analysis is performed manual in 6 different regions of the investigated substrates.

Results obtained by optical microscopy have shown reasonable cell attachment in all four samples type presented. However, due to low sample size and inability of imaging bulk Si, I have used a commercially available assay to quantify cell viability and proliferation, discussed in detail in following section. Figure 4.3 shows bottom-up bright field imaging of 3T3 fibroblasts cultured on,220 nm Si/Hybrid PDMS (1:10) was performed at 3, 5 days in vitro.

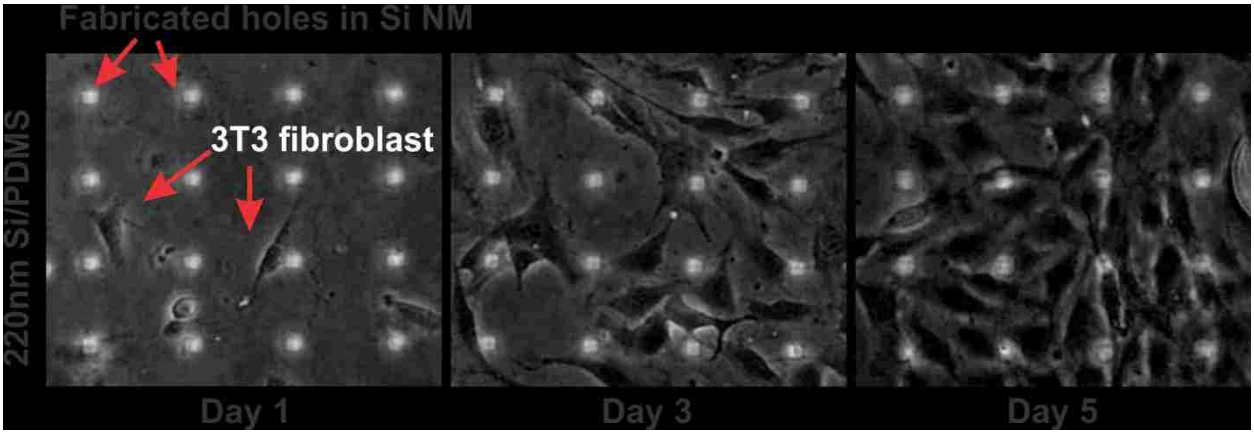

Figure 4.3: Bright field optical images of 3T3 fibroblast cultured *in vitro* on a fabricated specimen including a 220 nm Si NM/PDMS. The Si NM is perforated with an array of 2D holes. The images were acquired using an inverted microscope over (1-5) days *in vitro* (DIV). The images clearly show a healthy proliferation of the cells on investigated surfaces over the course of study, thereby confirming the viability of 3T3 fibroblasts on the fabricated specimens.

Results: Cell viability and cell proliferation using flow cytometry

All samples studied using flow cytometry are sterilized by autoclave and functionalized using UV ozone plasma facilitating similar surface functional groups; eliminating effects of surface chemistry (see Ch. 2 for additional details on UV ozone plasma). 3T3s are seeded at a density of ~25,000 cells/well on various samples namely, bulk Si, bare PDMS/hybrid (1:20) and SiNM 220nm on hybrid (1:20). Samples are placed in a 24-well plate flask with 1.5 cm diameter well. Fabricated ECLS is a 1 cm^2 x1 cm^2 lateral size NM with perforation of 5μm holes spaced 60μm apart, transferred on a hybrid (1:20) PDMS. ECLS, bulk silicon and bare PDMS are tailored to fit the culture well. The Alexa Fluor® 488 annexin V/Dead Cell Apoptosis Kit with Alexa® Fluor 488 annexin V and PI for flow cytometry is employed to classify cultured cell population into live and dead cells; specifically, apoptotic cells are labeled with green fluorescence; dead cells with red fluorescence, and live cells with little or no fluorescence. Cell population is then distinguished using a 488 nm line of an argon-ion laser for excitation. Control experiment determines gates used to exclude debris. Detailed experimental procedures are described in chapter 2. Figure 4.3, shows proliferation of 3T3 fibroblast on ECLS platform (220nm/hybrid (1:20)). The graph in figure 4.4 shows the viability values (i.e. the number of living cells in percentage on a particular sample for a definite time point) of 3T3 fibroblast on three different substrates. For a material to be considered safe and biologically acceptable there should be little to no apoptosis which implies the living cell population on a substrate should be over 70%. From the graph, we can see that the viability values for days 0-7 range from 75% – 92%, well beyond the safe range. Bulk silicon and ECLS (220nm/hybrid (1:20)) have promoted more initial cell attachment and viability then that of PDMS. Owing to UVO treatment of all samples, I assume same function group at the surface of PDMS, bulk silicon and SiNM/PDMS, in which case the lesser

initial attachment of 3T3 fibroblast on PDMS can be solely attributed to stiffness of substrate. The most important take away from this result is, ECLS have promoted heathy cell growth over the course of experiment; the specific stiffness impact on 3T3 fibroblast on Si substrate with varying mechanical properties is studied in next section using ICC staining of cells.

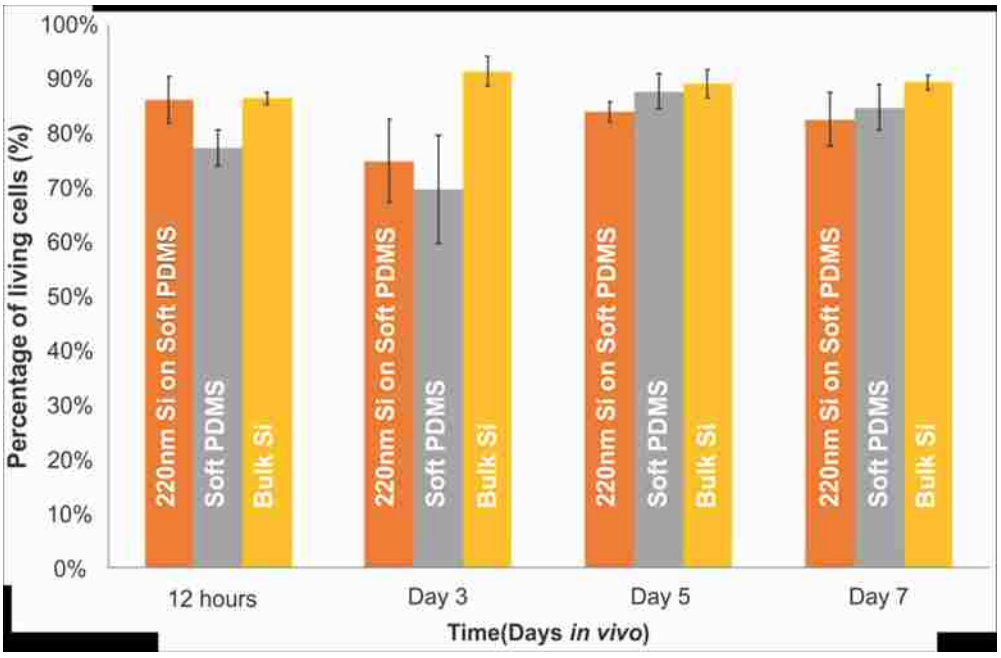

Figure 4.4: Living cell population of 3T3 fibroblast at four specific time periods; if a substrate reads 70% or more living cells, substrate is considered to be biocompatible

Figure 4.5 is a graph referred to as growth curve or cell proliferation curve, with time in culture media on X-axis and cell count on Y-axis. Essentially, living cell population for each time point obtained from flow cytometry is plotted with respect to culture time. In general, a healthy cell growth on a substrate is expected to have a generic trend of exponential growth over time. Here, 3T3 fibroblast are initially seeded at 25,000 cells/well cultured on three different substrates namely; ECLS (SiNM 220nm on PDMS), bulk silicon and hybrid (1:20) PDMS. I consider

performance of bulk silicon to be similar to that of standard tissue culture substrate i.e. polystyrene TCPS. 3T3 fibroblasts had shown statistically significant impact on the cell growth on substrate with elastic modulus less than 10 kPa gels after 24 and 48 h, respectively. Here, the stiffness of the ECLS is in range of more than 100kpa. Therefore, stiffness influence on rate of the proliferation suggests cells experience relatively similar stiffness on ECLS (220nm/hybrid (1:20) PDMS) compared to that of rigid silicon wafer which is understandable as SiNM 220nm is stiff (Refer section on Nanoindentation). Graph shows all the substrate attains confluent culture at day 7. All three substrates used to analyze the number of cells on the substrates resulted in observation of the standard trends throughout the study. The standard deviation for all substrate increases with culture time. The bulk silicon substrate by the end had greatest standard deviation. The large standard deviation is associated with the clustering of cells as cell density increased.

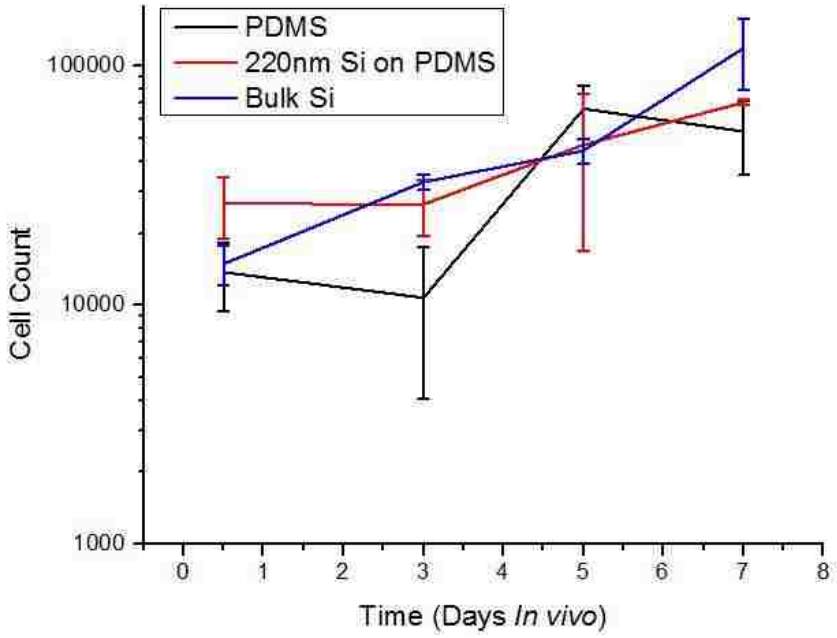

Figure.4.5. Growth curve associated with three different samples with drastic change in elastic modulus; SiNM/PDMS (approx. 160kPa); bare PDMS (approx. 80kPa) and bare silicon (approx. 164 GPa). Number of viable cells stained with CyQuant Direct Cell Proliferation assay measured with flow cytometer.

Results: Actin Cytoskeleton and Focal Adhesion

3T3 fibroblast cell structure is reported to show evident effects of substrate rigidity, particularly, F-actin fibers and focal adhesions points. To study change in cell structure on fabricated substrates, I have used immunofluorescent staining of cytoskeleton containing specific fluorescent-label to map local orientation of actin filaments within cell and a monoclonal antibody to stain focal contacts in cells. Confocal fluorescence microscopy was used to detect any alteration in shape and size of 3T3 fibroblast with respect to substrates with dissimilar mechanical properties. Specifically, the isolated cell response is evaluated from stress fiber organization and focal adhesions.

Results presented in Figure 4.6 show 3T3 fibroblast on bulk Si, 220 nm Si/Soft PDMS (i.e. hybrid (1:20) PDMS) and <20 nm Si/Soft PDMS. The surface chemistry of the selected culture platforms is identical. On the other hand, the effective elastic moduli of the three substrates are dramatically different; as a result, change in cells response is solely attributed to mechanical cues of culture substrate. In each figure, the representative cell shape, size and orientation of 3T3 on different substrates is captured. Figure 4.6.a shows 3T3 fibroblasts on bulk Si, 3T3s on silicon were observed to have a large cell size and wide spread which is expected of 3T3s cultured on stiff substrates (see section on 3T3s fibroblast typical behavior). Fig 4.6.b shows cells on ECLS comprising 220 nm Si on soft PDMS (i.e. hybrid (1:20). We can see reduction in cell spread area on this substrate. Fig 4.6.c has ECLS with silicon < 20nm on hybrid (1:20) PDMS, approx. 80kPa elastic modulus. Here we see a significant change in cell shape and spread area of 3T3s, which is expected of 3T3s cultured on soft substrate.

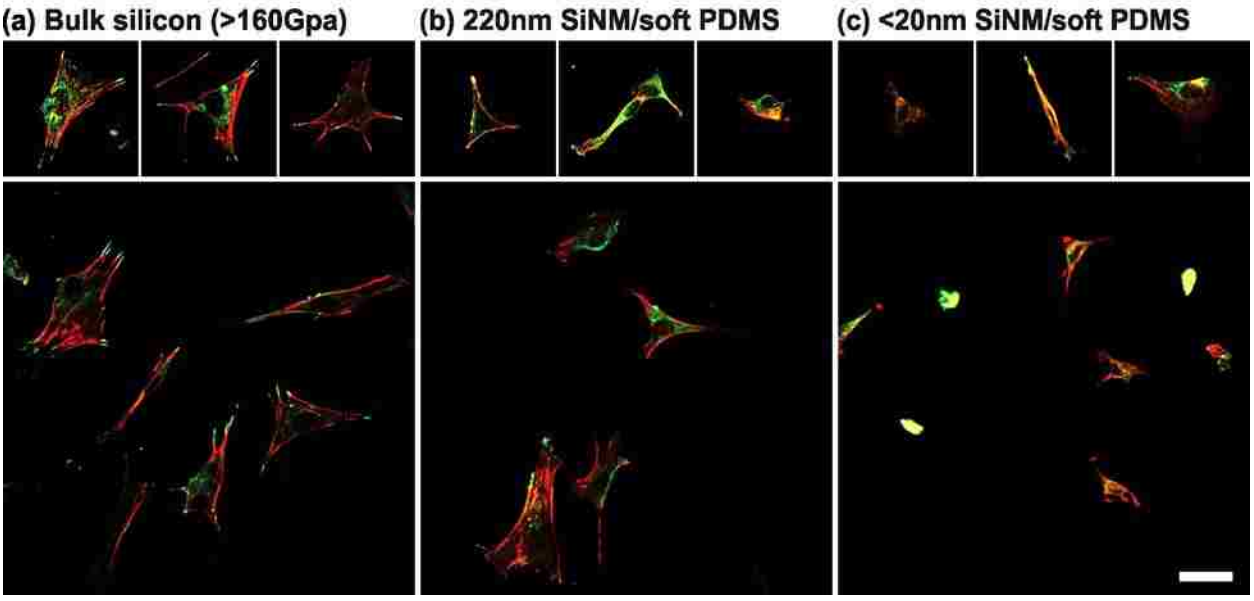

Figure.4.6. illustrate 3T3 fibroblast change in size, shape and orientation with respective mechanical properties of substrate. a) Bulk silicon (in Gpa range). b) Hard ECLS composed of SiNM 220nm on PDMS hybrid (1:20), elastic modulus approx. 160kPa c) soft ECLS with Si NM 20nm on hybrid PDMS (1:10) elastic modulus approx. 80kpa.

I have also investigated stress fiber organization and focal adhesion of isolated cells on bulk Si, 220 nm Si/Soft PDMS, and <20 Si/soft PDMS. Confocal microscopy images are shown in Fig. 4.7 displays cells stained for cytoskeleton. 3T3 fibroblasts culture on bulk Si and 220nm Si/PDMS have distinct stress fiber organization and elongated stable focal adhesion points as shown in fig 4.7.a. and 4.7.b. Figure 4.7.c shows 3T3 fibroblast on <Si 20 nm/PDMS. Fiber organization on this substrate was barely in detectable levels and also diffused adhesion points were observed. We see significant change in structure definition between a bare Si and a soft ECLS substrate. The 3T3 behavior observed here on ECLS (<20nm) with elastic modulus of 80 kPa is in line with what is expected from 3T3 fibroblast response on soft substrates.

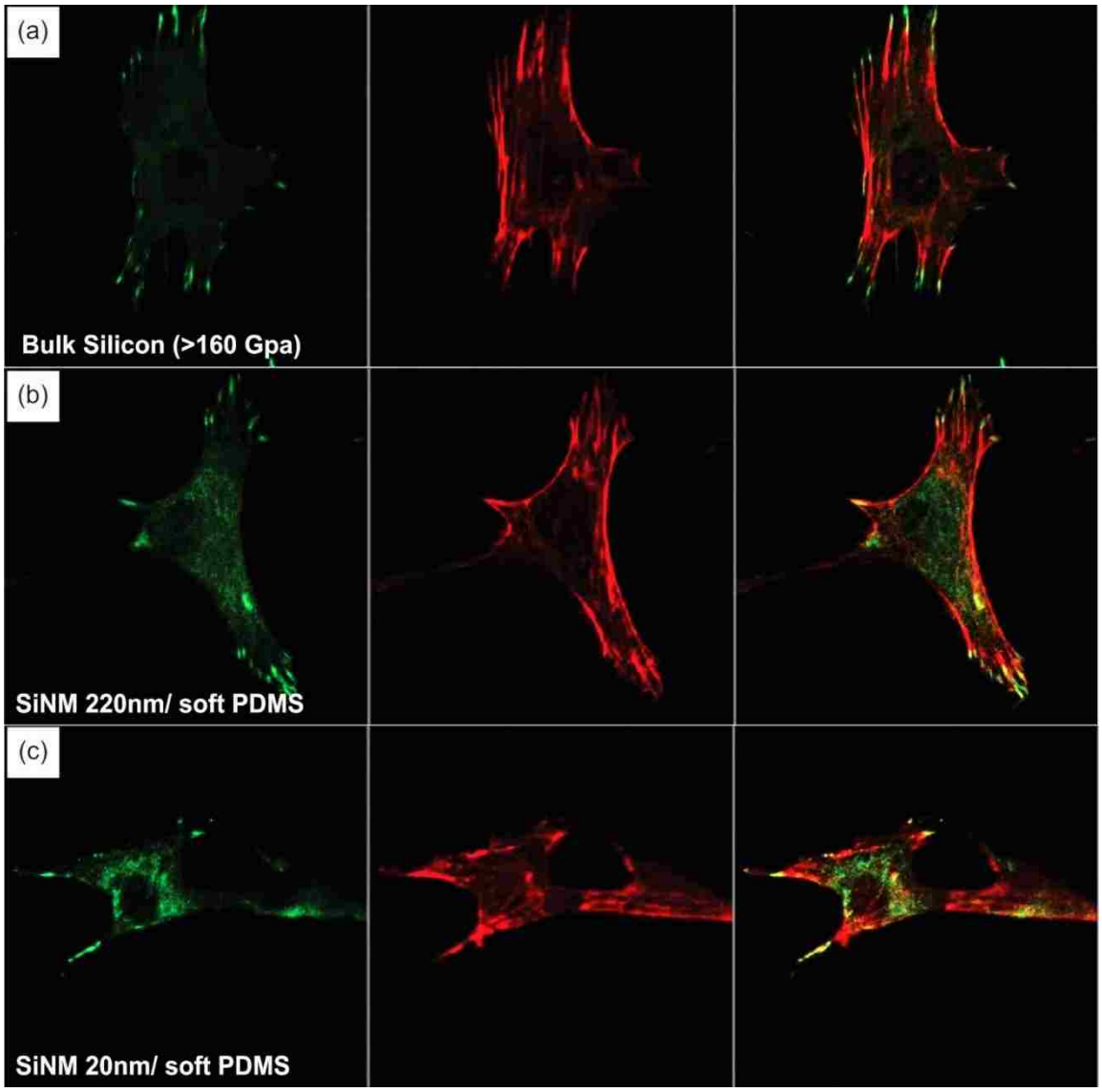

Figure 4.7: Single cell focal attachment points and F- actin fiber organization on substrates with different mechanical properties. a) 3T3 fibroblast on bare silicon wafer (Elastic modulus approx. 140Gpa). b) hard ECLS comprised of SiNM 220nm on PDMS hybrid (1:20), elastic modulus approx. 160kPa. c) soft ECLS with Si NM 20nm on hybrid PDMS (1:20) elastic modulus approx. 80kpa.

A significant difference in fiber organization between bulk Si and soft ECLS can be seen, unorganized and unstable fiber organization in 3T3 fibroblast are characteristic of its behavior on soft substrate. The 3T3 on the Hard ECLS had

little stress fiber organization compared to that of soft ECLS. However, on softest ECLS never to no stress fiber organization was observed which is similar to that of bare PDMS.

Chapter 5: Summary and Future directions

Summary

In this thesis, an Effectively Compliant Layered Substrate (ECLS) approach was proposed to address the issue of mechanical mismatch between cell-device microenvironment. I have successfully implemented the technique to engineer various Si-based ECLS platform with dissimilar mechanical properties using nano-fabrication technology. Ideological reasoning for using such approaches and length scales essentially was to acknowledge the drastic change in mechanical properties of an intrinsically rigid substrate in the range of three orders of magnitude accomplished just by moving from bulk material to nanomembrane. This thesis was divided into three main sections, each of which focused on a particular aspect of the ECLS.

The first section of the thesis aimed at synthesis of a biocompatible, chemically and mechanically stable compliant substrate as support base for ECLS platform. In order to achieve this, various PDMS formulations were developed to fabricate compliant base with elastic modulus in the ranges of kPa. Wetting properties of the polymer stamp were improved by UVO treatment to promote healthy bioactivity. In final stage, the compliant substrates created by this method were seamlessly translated into various ECLS platforms.

In the second portion of this thesis various configurations of SiNM were realized using a technique called TSP approach namely, thinning, shaping, and perforating. The idea was to see the extent to which mechanical properties of silicon in nanoscale can be tailored. In order to do so, SiNM of various thicknesses were transferred on to a compliant base with similar mechanical properties. Bilayers were characterized using nano-indentation to meausure effective elastic modulus of

substrates. It was demonstrated that SiNM in tens of nanometer thickness replicates mechanical properties similar to that of its compliant base

In the third portion of this thesis, *In-vitro* cell study was conducted using 3T3 fibroblast cell line to test cell viability and cell growth on ECLS platforms. Additionally, cell expressions like fiber organization and focal adhesion were used as indication of change in mechanical properties of fabricated platforms. The results show a significant difference in cell behavior at different levels. 3T3s were observed to change shape, size, and expression corresponding to change in mechanical properties.

In conclusion, by implementing proposed techniques, I was able to fabricate a combination of robust and reliable non-biodegradable silicon electronics material based compliant platforms which offers both the flexibility of the device and sufficient bulk degradation that the immune response to the remaining material is minimal. Proposed ECLS have offered exceptional biocompatibility and mechanical sensitivity. In addition, ECLS approach makes non transparent bulk silicon into an optical transparent platform allowing bright field imaging in tissue culture environment. The next generation of ECLS promises more efficient and comprehensive bio-device integration. Proposed compliant culture platforms can find immediate application in clinical research for therapeutic strategies in wound healing and tissue engineering.

Future directions

- As it can be seen from this chapter, much progress has been made in controlling mechanical properties of ECLS by tailoring compliant base and functional layer. One direction for future work can be study of different type of cells; especially study of neuronal cell on fabricated substrates with device functionality may revolutionize *in vitro* study of neuronal cells.
- The next obvious step is the characterization of electronic and photonic response of ECLS platforms in tissue culture. Figure 5.1 shows a schematic of proposed process flow to facilitate device functionality.

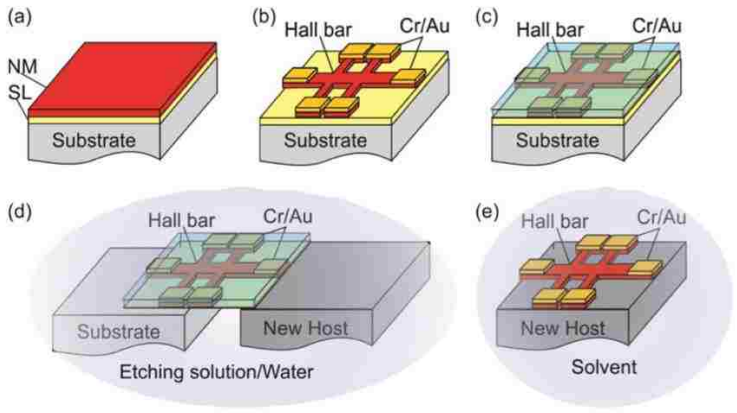

Figure 5.1: Hall bar fabrication, release and transfer on the compliant substrate. Hall bars are fabricated on the unreleased NM by conventional top-down processing techniques (a)-(b). A support layer is spun onto the fabricate device (c) to provide mechanical stability during release and transfer to the compliant host (d). The support layer is finally cleaned by solvents (e).

- Another direction for future work is to investigate stable compliant base in the range of approx. 20kPa or less, such that it facilitates easy ECLS fabrication. Despite significant progress presented in this thesis, to distinguish drastic cell expressions, common studies in mechanobiology employ hydrogels for a wide variety of biological tissue. Compliant base elastic modulus used in this study can be further decreased by varying the

ratio of 184 kits in the hybrid blend of 184:527 from standard 10parts base to 1part curing agent to (20:1); (30:1) and (50:1). However, this might increase the possibility of more loose oligomers with increased dilution, extra time in solvent extraction should help.

- Lastly, in the view of creating more relevant biological condition on-chip, device graded substrates should be investigated as a platform for 3D cell culture by facilitating 3D microstructures on ECLS platforms. The work would include realization of 3D scaffolds on ECLS and their integration in tissue culture with device functionality. Figure 5.2 shows fabricated 3D microstructures on ECLS. Out of plane microstructures on ECLS were realized by following the process of guided-self-assembly procedure. Primarily, NM is designed with organized stress concentrators. The adhesion energies between the bi-layers are manipulated. Finally, by controlled compressive stress induction and eventual stress relaxation I realize 3D microstructures on ECLS.

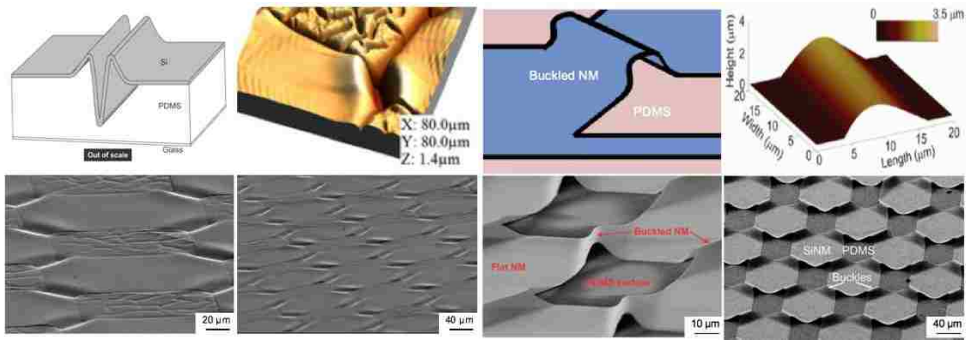

Figure 5.2: a) Groove like 3D microstructure on ECLS. b) Buckle like 3D microstructure on ECLS

Reference

1) ***Fissell, W.H.; Fleischman, A.J.; Humes, H.D.; Roy, S. Development of continuous implantable renal replacement: past and future. Transl. Res. 2007, 150, 327–336.***
2) ***Fissell, W.H.; Manley, S.; Westover, A.; Humes, H.D.; Fleischman, A.J.; Roy, S. Differentiated growth of human renal tubule cells on thin-film and nanostructured materials. ASAIO J. 2006, 52, 221–227.***
3) ***Salonen, J.; Kaukonen, A.M.; Hirvonen, J.; Lehto, V.P. Mesoporous silicon in drug delivery applications. J. Pharm. Sci. 2008, 97, 632–653.***
4) ***Anglin, E.J.; Cheng, L.; Freeman, W.R.; Sailor, M.J. Porous silicon in drug delivery devices and materials. Adv. Drug. Deliv. Rev. 2008, 60, 1266–1277.***
5) ***Canham, L.T. Bioactive silicon structure fabrication through nanoetching techniques. Adv. Mater. 1995, 7, 1033–1037.***
6) ***Whitesides, G.M.; Ostuni, E.; Takayama, S.; Jiang, X.; Ingber, D.E. Soft lithography in biology and biochemistry. Annu. Rev. Biomed. Eng. 2001, 3, 335–373.***
7) ***Xia, Y.N.; Whitesides, G.M. Soft lithography. Annu. Rev. Mater. Sci. 1998, 28, 153–184.***
8) ***Makamba, H.; Kim, J.H.; Lim, K.; Park, N.; Hahn, J.H. Surface modification of poly(dimethylsiloxane) microchannels. Electrophoresis 2003, 24, 3607–3619.***
9) ***Mirzadeh, H.; Shokrolahi, F.; Daliri, M. Effect of silicon rubber crosslink density on fibroblast cell behavior in vitro. J. Biomed. Mater. Res. A 2003, 67, 727–732.***
10) ***Ali Khademhosseini. Nanoscale and Microscale Approaches for Engineering the in vitro Cellular Microenvironment***
11) ***Leclerc, E.; Sakai, Y.; Fujii, T. Perfusion culture of fetal human hepatocytes in microfluidic environments. Biochem. Eng. J. 2004, 20, 143–148.***
12) ***Ostrovidov, S.; Jiang, J.L.; Sakai, Y.; Fujii, T. Membrane-based PDMS microbioreactor for perfused 3D primary rat hepatocyte cultures. Biomed. Microdev. 2004, 6, 279–287.***
13) ***Berit Brockmeyer1 & Uta R. Kraus1 & Norbert Theobald1. Accelerated solvent extraction (ASE) for purification and extraction of silicone passive samples.***
14) ***Irena Barbulovic-Nad New Microfludic Platform for Cell studies.***
15) ***Chetan Bhuwania. Substrate Stiffness Adustable PDMS Device/Array for Understanding Its Effects on Cell Growth, Differencation and Migration***
16) ***Ming Ni 1, Wen Hao Tong 1,2, Deepak Choudhury 1,2, Nur Aida Abdul Rahim 3, Ciprian Iliescu 1,* and Hanry Yu 1,2,3,4,5- Cell Culture on MEMS Platforms: A Review***
17) ***Chun-Min Lo,* Hong-Bei Wang,* Micah Dembo,† and Yu-li Wang* Cell Movement Is Guided by the Rigidity of the Substrate***
18) ***Anna M Clausen. Using Silicon Nanomembranes to Evaluate Stress in Deposited Thin Films***
19) ***Arnold Melvin Kiefer. Silicon/Germanium Junctions Formed by Membrane bonding.***
20) ***Tony Yeung,1 Penelope C. Georges,1 Lisa A. Flanagan,2 Beatrice Marg,2 Miguelina Ortiz,1 Makoto Funaki,1 Nastaran Zahir,1 Wenyu Ming,1 Valerie Weaver,1 and Paul A. Janmey1,2* Effects of Substrate Stiffness on Cell Morphology, Cytoskeletal Structure, and Adhesion***

21) *Nan Sun¶,*, Yong Liu#, Ling Qin§, Guangyu Xu§, and Donhee Ham§,* Solid-State and Biological Systems Interface*
22) *Francesca Cavallo and Max G Lagally* Semiconductor nanomembranes: a platform for new properties via strain engineering*
23) *Francesca Cavallo* and Max G. Lagally Semiconductors turn soft: inorganic nanomembranes*
24) *Je´roˆme Solon,*y Ilya Levental,*z Kheya Sengupta,*{ Penelope C. Georges,*z and Paul A. Janmey*§ Fibroblast Adaptation and Stiffness Matching to Soft Elastic Substrates*
25) *Masha Prager-Khoutorsky1,4,5, Alexandra Lichtenstein1,4, Ramaswamy Krishnan2,5, Kavitha Rajendran2,5, Avi Mayo1, Zvi Kam1, Benjamin Geiger1,6 and Alexander D. Bershadsky1,3,6 Fibroblast polarization is a matrix-rigidity-dependent process controlled by focal adhesion mechanosensing*
26) *W.C. Oliver G.M. Pharra Measurement of hardness and elastic modulus by instrumented indentation: Advances in understanding and refinements to methodology*
27) *Michelle M. Kelly Elastic Strain Sharing in Silicon/Silicon Germanium Nanomembrane.*
28) *Sara Molladavoodi Investigating Mechanical Interactions of Cells with Their Environment*
29) *Minghuang Huang,*a Francesca Cavallo,a Feng Liub and Max G. Lagallya Nanomechanical architecture of semiconductor nanomembranes*
30) *Deborah Marie Paskiewicz Elastic Strain Engineering in Silicon and Silicon-Germanium Nanomembranes*
31) *Zhixin Wang Polydimethylsiloxane Mechanical Properties Measured by Macroscopic Compression and Nanoindentation Techniques*
32) *Kirill Efimenko,* William E. Wallace,† and Jan Genzer*, 1Surface Modification of Sylgard-184 Poly(dimethyl siloxane) Networks by Ultraviolet and Ultraviolet/Ozone Treatment*
33) *J. A. Rogers1, M. G. Lagally2 & R. G. Nuzzo3 Synthesis, assembly and applications of semiconductor nanomembranes*
34) *Matthew N. Rush1,2, Kent E. Coombs1,3, and Elizabeth L. Hedberg-Dirk1,2,4*. Surface Chemistry Regulates Valvular Interstitial Cell Differentiation In Vitro*
35) *Fut K. Yang, Wei Zhang, Yougun Han, Serge Yoffe, Yungchi Cho, and Boxin Zhao* "Contact" of Nanoscale Stiff Films*
36) *Li-Heng Cai, Thomas E. Kodger, Rodrigo E. Guerra, Adrian F. Pegoraro, Michael Rubinstein,* and David A. Weitz* Soft Poly(dimethylsiloxane) Elastomers from Architecture- Driven Entanglement Free Design*
37) *Jessica M. Dechene Surface Modi cations of Poly(dimethylsiloxane) for Biological Application of Micro uidic Devices*
38) *Qian Wang Elastomer-based Cellular Micromechanical Stimulators for Mechanobiological Study*
39) *Dennis E. Discher,1* Paul Janmey,1 Yu-li Wang2 Tissue Cells Feel and Respond to the Stiffness of Their Substrate*
40) *Christine E. Schmidt1 and Jennie Baier Leach2 NEURAL TISSUE ENGINEERING: Strategies for Repair and Regeneration*

41) *A. Evren Özçam 1, Kirill Efimenko, Jan Genzer* Effect of ultraviolet/ozone treatment on the surface and bulk properties of poly(dimethyl siloxane) and poly(vinylmethyl siloxane) networks*
42) *Francesca Cavallo,* Kevin T Turner1, and Max G Lagally Facile Fabrication of Ordered Crystalline-Semiconductor Microstructures on Compliant Substrates*
43) *[W. P. Dumke, J. M. Woodall, and V. L. Rideout "GaAs-GaAlAs Heterojunction Transistor for High Frequency Operation" Solid-State Electronics 15 (1972) 1339─1343*
44) *B. A. Irving "The Preparation of Thin Films of Germanium and Silicon" British Journal of Applied Physics 12 (1961) 92─93*
45) *M. Bruel "Silicon on Insulator Material Technology" Electronics Letters 31 (1995) 1201─1202*
46) *O. Moutanabbir and U. Gösele "Heterogeneous Integration of Compound Semiconductors" Annual Review of Materials Research 40 (2010) 469—500.*
47) *D. J. Monk, D. S. Soane, and R. T. Howe "Hydrofluoric Acid Etching of Silicon Dioxide Sacrificial Layers: II. Modeling" Journal of the Electrochemical Society 141 (1994) 270 – 274*
48) *J. Bühler, F.-P. Steiner, and H. Baltes "Silicon Dioxide Sacrificial Layer Etching in Surface Micromachining" Journal of Micromechanical Machining 7 (1997) R1 – R13*
49) *K. R. Williams, K. Gupta, and M. Wasilik "Etch Rates for Micromachining Processing—Part II" Journal of Microelectromechanical Systems 12 (2003) 761 – 778*
50) *in Ge and Associated Defect Control" Journal of Electrochemical Society 153 (2006) G229 – G233 Adams CL, Nelson WJ. 1998. Cytomechanics of cadherin-mediated cell-cell adhesion. Curr Opin Cell Biol 10:572–577.*
51) *Balaban NQ, Schwarz US, Riveline D, Goichberg P, Tzur G, Sabanay I, Mahalu D, Safran S, Bershadsky A, Addadi L, Geiger B. 2001. Force and focal adhesion assembly: a close relationship studied using elastic micropatterned substrates. Nat Cell Biol 3:466 – 472.*
52) *Bao G, Suresh S. 2003. Cell and molecular mechanics of biological materials. Nat Mater 2:715–725.*
53) *Bard JB, Hay ED. 1975. The behavior of fibroblasts from the devel- oping avian cornea. Morphology and movement in situ and in vitro. J Cell Biol 67:400–418.*
54) *Cunningham CC, Vegners R, Bucki R, Funaki M, Korde N, Hartwig JH, Stossel TP, Janmey PA. 2001. Cell permeant polyphosphoi- nositide-binding peptides that block cell motility and actin assembly. J Biol Chem 276:43390–43399.*
55) *Danjo Y, Gipson IK. 1998. Actin "purse string" filaments are anchored by E-cadherin-mediated adherens junctions at the leading edge of the epithelial wound, providing coordinated cell movement. J Cell Sci 111:3323–3332.*
56) *Rogers JA, Lagally MG, Nuzzo RG: Semiconductor nanomembranes: synthesis, assembly, and applications. Nature 2011, 477:45.*
57) *Ahn JH, Kim HS, Lee KJ, Jeon S, Kang SJ, Sun Y, Nuzzo RG, Rogers JA:*
58) *Heterogeneous three-dimensional electronics by use of printed*
59) *Semiconductor nanomaterials. Science 2006, 314:1754. 3. Khang DY, Jiang HQ, Huang Y, Rogers JA: A stretchable form of single- crystal silicon for high-performance electronics on rubber substrates.*

60) Science 2006, 311:208. 4. Roberts MM, Klein LJ, Savage DE, Slinker KA, Friesen M, Celler GK, Eriksson
61) MA, Lagally MG: Elastically relaxed free-standing strained-silicon
62) nanomembranes. Nat Mater 2006, 5:388.
63) D. Tabor, Review of Physics in Technology, 1970, 1, 145–179.
64) Membrane Handbook, ed. W. S. W. Ho and K. K. Sikar, Chapman and Hall, New York, 1992.
65) J. Li, M. Gershow, D. Stein, E. Brandin and J. A. Golovchenko, Nat. Mater., 2003, 2, 611–615.
66) M. G. N. Fertig, M. Klau, R. H. Blick and J. C. Behrends, Appl. Phys. Lett., 2002, 81, 4865–4867.
67) M. M. Roberts, L. J. Klein, D. E. Savage, K. A. Slinker, M. Friesen, G. K. Celler, M. A. Eriksson and M. G. Lagally, Nat. Mater., 2006, 5, 388–393.
68) S. A. Scott and M. G. Lagally, J. Phys. D: Appl. Phys., 2007, 40, R75– R92.
69) N. Bowden, S. Brittain, A. G. Evans, J. W. Hutchinson and G. M. Whitesides, Nature, 1998, 393, 146–149.
70) J. Huang, M. Juszkiewicz, W. H. de Jeu, E. Cerda, T. Emrick, N. Menon and T. P. Russell, Science, 2007, 317, 650–653.
71) F. Liu, P. Rugheimer, E. Mateeva, D. E. Savage and M. G. Lagally, Nature, 2002, 416, 498.
72) Y. Mei, D. J. Thurmer, F. Cavallo, S. Kiravittaya and O. G. Schmidt, Adv. Mater., 2007, 19, 2124–2128.
73) M. Huang, C. Boone, M. M. Roberts, D. E. Savage, M. G. Lagally, N. Shaji, H. Qin, R. Blick, J. A. Nairn and F. Liu, Adv. Mater., 2005, 17, 2860–2864.
74) Levental, I., P. C. Georges, and P. A. Janmey. 2007. Soft biological materials and their impact on cell function. Soft Matter. 1:299–306.
75) Engler, A. J., S. Sen, H. L. Sweeney, and D. E. Discher. 2006. Matrix elasticity directs stem cell lineage specification. Cell. 126:677–689.
76) Pelham, R. J., Jr., and Y. Wang. 1997. Cell locomotion and focal adhe- sions are regulated by substrate flexibility. Proc. Natl. Acad. Sci. USA. 94:13661–13665.
77) Discher, D. E., P. Janmey, and Y. L. Wang. 2005. Tissue cells feel and respond to the stiffness of their substrate. Science. 310:1139–1143.
78) Georges, P. C., and P. A. Janmey. 2005. Cell type-specific response to growth on soft materials. J. Appl. Physiol. 98:1547–1553.
79) Yeung, T., P. C. Georges, L. A. Flanagan, B. Marg, M. Ortiz, M. Funaki, N. Zahir, W. Ming, V. Weaver, and P. A. Janmey. 2005. Effects of substrate stiffness on cell morphology, cytoskeletal structure, and adhesion. Cell Motil. Cytoskeleton. 60:24–34.
80) Paszek, M. J., N. Zahir, K. R. Johnson, J. N. Lakins, G. I. Rozenberg, A. Gefen, C. A. Reinhart-King, S. S. Margulies, M. Dembo, D. Boettiger, D. A. Hammer, and V. M. Weaver. 2005. Tensional homeostasis and the malignant phenotype. Cancer Cell. 8:241–254.

81) Engler, A., L. Bacakova, C. Newman, A. Hategan, M. Griffin, and D. Discher. 2004. Substrate compliance versus ligand density in cell on gel responses. Biophys. J. 86:617–628.

82) Pourati, J., A. Maniotis, D. Spiegel, J. L. Schaffer, J. P. Butler, J. J. Fredberg, D. E. Ingber, D. Stamenovic, and N. Wang. 1998. Is cytoskeletal tension a major determinant of cell deformability in adherent endothelial cells? Am. J. Physiol. Cell Physiol. 274:C1283– 1289.

83) Chrzanowska-Wodnicka, M., and K. Burridge. 1996. Rho-stimulated contractility drives the formation of stress fibers and focal adhesions. J. Cell Biol. 133:1403–1415.

84) Engler AJ, Sen S, Sweeney HL, Discher DE (2006) Matrix elasticity directs stem cell lineage specification. Cell 126: 677–689.

85) Pelham RJ Jr, Wang Y (1997) Cell locomotion and focal adhesions are regulated by substrate flexibility. Proc Natl Acad Sci U S A 94: 13661–13665.

86) Discher DE, Janmey P, Wang YL (2005) Tissue cells feel and respond to the stiffness of their substrate. Science 310: 1139–1143.

87) Discher DE, Engler A, Carag C, Rehfeldt F (2008) Matrix elasticity effects on cardiomyocytes and stem cells: Similarities, differences and therapeutic implications. Biorheology 45: 54–54.

88) Engler AJ, Carag-Krieger C, Johnson CP, Raab M, Tang HY, et al. (2008) Embryonic cardiomyocytes beat best on a matrix with heart-like elasticity: scar- like rigidity inhibits beating. Journal of Cell Science 121: 3794–3802.

89) Chowdhury F, Li Y, Poh Y-C, Yokohama-Tamaki T, Wang N, et al. (2010) Soft Substrates Promote Homogeneous Self-Renewal of Embryonic Stem Cells via Downregulating Cell-Matrix Tractions. PLoS One 5: e15655.

90) Zoldan J, Karagiannis ED, Lee CY, Anderson DG, Langer R, et al. (2011) The influence of scaffold elasticity on germ layer specification of human embryonic stem cells. Biomaterials 32: 9612–9621.

91) 1. W.C. Oliver and G.M. Pharr, J. Mater. Res. 7, 1564 (1992).

92) G.M. Pharr, W.C. Oliver, and F.R. Brotzen, J. Mater. Res. 7, 613 (1992).

93) J.B. Pethica, R. Hutchings., and W.C. Oliver, Philos. Mag. A 48, 593 (1983).

94) F. Frolich, P. Grau, and W. Grellmann, Phys. Status Solidi 42, 79 (1977).

95) D. Newey, M.A. Wilkins, and H.M. Pollock, J. Phys. E: Sci. In- strum. 15, 119 (1982).

96) G.M. Pharr and W.C. Oliver, MRS Bull. 17, 28 (1992).

97) G.M. Pharr, Mater. Sci. Eng. A 253, 151 (1998).

98) T.D. Shen, C.C. Koch, T.Y. Tsui, and G.M. Pharr, J. Mater. Res. 10, 2892 (1995).

D. Stone, W.R. LaFontaine, P. Alexopoulos, T.W. Wu, and C-Y. Li, J. Mater. Res. 3, 141 (1988).